The Legacy of Bernhard Riemann
After One Hundred and Fifty Years
ALM 35, pp. 417–457

The Riemann Minimal Examples

William H. Meeks III, Joaquín Pérez

Abstract

Near the end of his life, Bernhard Riemann made the marvelous discovery of a 1-parameter family R_λ, $\lambda \in (0, \infty)$, of periodic properly embedded minimal surfaces in $\mathbb{R}^3$ with the property that every horizontal plane intersects each of his examples in either a circle or a straight line. Furthermore, as the parameter $\lambda \to 0$ his surfaces converge to a vertical catenoid and as $\lambda \to \infty$ his surfaces converge to a vertical helicoid. Since Riemann's minimal examples are topologically planar domains that are periodic with the fundamental domains for the associated $\mathbb{Z}$-action being diffeomorphic to a compact annulus punctured in a single point, then topologically each of these surfaces is diffeomorphic to the unique genus zero surface with two limit ends. Also he described his surfaces analytically in terms of elliptic functions on rectangular elliptic curves. This article exams Riemann's original proof of the classification of minimal surfaces foliated by circles and lines in parallel planes and presents a complete outline of the recent proof that every properly embedded minimal planar domain in $\mathbb{R}^3$ is either a Riemann minimal example, a catenoid, a helicoid or a plane.

2000 Mathematics Subject Classification: Primary 53A10 Secondary 49Q05, 53C42, 57R30.

Keywords and Phrases: Minimal surface, Shiffman function, Jacobi function, Korteweg-de Vries equation, KdV hierarchy, minimal planar domain.

Contents

1 Introduction

Shortly after the death of Bernhard Riemann, a large number of unpublished handwritten papers were found in his office. Some of these papers were unfinished, but all of them were of great interest because of their profound insights and because of the deep and original mathematical results that they contained. This discovery of Riemann's handwritten unpublished manuscripts led several of his students and colleagues to rewrite these works, completing any missing arguments, and then to publish them in their completed form in the Memoirs of the Royal Society of Sciences of Göttingen as a series of papers that began appearing in 1867.

One of these papers [37], written by K. Hattendorf and M. H. Weber from Riemann's original notes from the period 1860-61, was devoted to the theory of minimal surfaces in $\mathbb{R}^3$. In one of these rewritten works, Riemann described several examples of compact surfaces with boundary that minimized their area among all surfaces with the given explicit boundary. In the last section of this manuscript Riemann tackled the problem of classifying those minimal surfaces which are bounded by a pair of circles in parallel planes, under the additional hypothesis that every intermediate plane between the planes containing the boundary circles also intersects the surface in a circle. Riemann proved that the only solutions to this problem are (up to homotheties and rigid motions) the catenoid and a previously unknown 1-parameter family of surfaces $\{R_\lambda \mid \lambda \in \mathbb{R}\}$, known today as the *Riemann minimal examples.* Later in 1869, A. Enneper [9] demonstrated that there do not exist minimal surfaces foliated by circles in a family of nonparallel planes, thereby completing the classification of the minimal surfaces foliated by circles.

This purpose of this article is threefold. Firstly we will recover the original arguments by Riemann by expressing them in more modern mathematical language (Section 4); more specifically, we will provide Riemann's analytic classification of minimal surfaces foliated by circles in parallel planes. We refer the reader to Figure 5 for an image of a Riemann minimal surface created from his mathematical formulas and produced by the graphics package in `Mathematica.` Secondly we will illustrate how the family of Riemann's minimal examples are still of great interest in the current state of minimal surface theory in $\mathbb{R}^3$. Thirdly, we will indicate the key results that have led to the recent proof that the plane, the helicoid, the catenoid and the Riemann minimal examples are the only properly embedded minimal surfaces in $\mathbb{R}^3$ with the topology of a planar domain; see Section 5 for a sketch of this proof. In regards to this result, the reader should note that the plane and the helicoid are conformally diffeomorphic to the complex plane, and the catenoid is conformally diffeomorphic to the complex plane punctured in a single point; in particular these three examples are surfaces of finite topology. However, the Riemann minimal examples are planar domains of infinite topology, diffeomorphic to each other and characterized topologically as being diffeomorphic to the unique

surface of genus zero with two limit ends. The proof that the properly embedded minimal surfaces of infinite topology and genus zero are Riemann minimal examples is due to Meeks, Pérez and Ros [30], and it uses sophisticated ingredients from many branches of mathematics. Two essential ingredients in their proof of this classification result are Colding-Minicozzi theory, which concerns the geometry of embedded minimal surfaces of finite genus, and the theory of integrable systems associated to the Korteweg-de Vries equation.

In 1956 M. Shiffman [39] generalized in some aspects Riemann's classification theorem; Shiffman's main result shows that a compact minimal annulus that is bounded by two circles in parallel planes must be foliated by circles in the intermediate planes. Riemann's result is more concerned with classifying analytically such minimal surfaces and his proof that we give in Section 4 is simple and self-contained; in Sections 4.2 and 5 we will explore some aspects of the arguments by Shiffman. After the preliminaries of Section 2, we will include in Section 3 the aforementioned reduction by Enneper from the general case in which the surface is foliated by circles to the case where the circles lie in parallel planes. In Section 4.1 we will introduce a more modern viewpoint to study the Riemann minimal examples, which moreover will allow us to produce graphics of these surfaces using the software package Mathematica. The analytic tool for obtaining this graphical representation will be the Weierstrass representation of a minimal surface, which is briefly described in Section 2.1. In general, minimal surfaces are geometrical objects that adapt well to rendering software, partly because from their analytical properties, the Schwarz reflection principle for harmonic functions can be applied. This reflection principle, that also explained in the preliminaries section, allows one to represent relatively simple pieces of a minimal surface (where the computer graphics can achieve high resolution), and then to generate the remainder of the surface by simple reflections or 180°-rotations around lines contained in the boundaries of the simple fundamental piece. On the other hand, as rendering software often represents a surface in space by producing the image under the immersion of a mesh of points in the parameter domain, it especially important that we use parameterizations whose associated meshes have natural properties, such as preserving angles through the use of isothermal coordinates.

Remark 1.1. There is an interesting dichotomy between the situation in $\mathbb{R}^3$ and the one in $\mathbb{R}^n$, $n \geq 4$. Regarding the natural n-dimensional generalization of the problem tacked by Riemann, of producing a family of minimal hypersurfaces foliated by $(n-2)$-dimensional spheres, W. C. Jagy [14] proved that if $n \geq 4$, then a minimal hypersurface in $\mathbb{R}^n$ foliated by hyperspheres in parallel planes must be rotationally symmetric. Along this line of thought, we could say that the Riemann minimal examples do not have a counterpart in higher dimensions.

Acknowledgements. The authors would like to express their gratitude to Francisco Martín for giving his permission to incorporate much of the material from a previous joint paper [19] by him and the second author into the present manuscript. In particular, the parts of our manuscript concerning the classical arguments of Riemann and Weierstrass are largely rewritten translations of the paper [19].

First author's financial support: This material is based upon work for the

NSF under Award No. DMS-1309236. Any opinions, findings, and conclusions or recommendations expressed in this publication are those of the authors and do not necessarily reflect the views of the NSF. Second author's financial support: Research partially supported by a MEC/FEDER grant no. MTM2011-22547, and Regional J. Andalucía grant no. P06-FQM-01642.

2 Preliminaries

Among the several equivalent defining formulations of a minimal surface $M \subset \mathbb{R}^3$, i.e., a surface with mean curvature identically zero, we highlight the Euler-Lagrange equation

$$(1+f_y^2)f_{xx} - 2f_x f_y f_{xy} + (1+f_x^2)f_{yy} = 0,$$

where M is expressed locally as the graph of a function $z = f(x,y)$ (in this paper we will use the abbreviated notation $f_x = \frac{\partial f}{\partial x}, \partial f_{xx}$, etc., to refer to the partial derivatives of any expression with respect to one of its variables), and the formulation in local coordinates

$$eG - 2fF + Eg = 0,$$

where $\begin{pmatrix} E & F \\ F & G \end{pmatrix}, \begin{pmatrix} e & f \\ f & g \end{pmatrix}$ are respectively the matrices of the first and second fundamental forms of M in a local parameterization. Of course, there are other ways of characterize minimality such as by the harmonicity of the coordinate functions or the holomorphicity of the Gauss map, but at this point it is worthwhile to remember the historical context in which the ideas that we wish to explain appeared. Riemann was one of the founders of the study of functions of one complex variable, and few things were well understood in Riemann's time concerning the relationship between minimal surfaces and holomorphic or harmonic functions. Instead, Riemann imposed minimality by expressing the surface in implicit form, i.e., by espressing it as the zero set of a smooth function $F\colon O \to \mathbb{R}$ defined in an open set $O \subset \mathbb{R}^3$, namely

$$\operatorname{div}\left(\frac{\nabla F}{|\nabla F|}\right) = 0 \quad \text{in } O, \tag{1}$$

where div and ∇ denote divergence and gradient in $\mathbb{R}^3$, respectively. The derivation of equation (1) is standard, but we next derive it for the sake of completeness. First note that

$$\operatorname{div}\left(\frac{\nabla F}{|\nabla F|}\right) = \frac{1}{|\nabla F|}\left(\Delta F - \frac{1}{|\nabla F|}(\nabla F)(|\nabla F|)\right),$$

where Δ is the laplacian on M; hence (1) follows directly from the next lemma.

Lemma 2.1. *If 0 is a regular value of a smooth function $F\colon O \to \mathbb{R}$, then the surface $M = F^{-1}(\{0\})$ is minimal if and only if $|\nabla F|\Delta F = (\nabla F)(|\nabla F|)$ on M.*

Proof. Since the tangent plane to M at a point $p \in M$ is $T_pM = \ker(dF_p) = \langle(\nabla F)_p\rangle^{\perp}$, then $(\nabla F)|_M$ is a nowhere zero vector field normal to M, and $N = (\frac{\nabla F}{|\nabla F|})|_M$ is a Gauss map for M. On the other hand,

$$\Delta F = \operatorname{trace}(\nabla^2 F) = \sum_{i=1}^{2} (\nabla^2 F)(E_i, E_i) + (\nabla^2 F)(N, N) \tag{2}$$

where $\nabla^2 F$ is the hessian of F and E_1, E_2 is a local orthonormal frame tangent to M. As $(\nabla^2 F)(E_i, E_i) = \langle E_i(\nabla F), E_i\rangle = \langle E_i(|\nabla F|N), E_i\rangle = |\nabla F|\langle dN(E_i), E_i\rangle$, then

$$\sum_{i=1}^{2} (\nabla^2 F)(E_i, E_i) = |\nabla F| \operatorname{trace}(dN) = -2|\nabla F|H, \tag{3}$$

with H the mean curvature of M with respect to N. Also, $|\nabla F|^2(\nabla^2 F)(N, N) = (\nabla^2 F)(\nabla F, \nabla F) = \frac{1}{2}(\nabla F)(|\nabla F|^2) = |\nabla F|(\nabla F)(|\nabla F|)$. Plugging this formula and (3) into (2), we get $|\nabla F|\Delta F = -2|\nabla F|^2 H + (\nabla F)(|\nabla F|)$, and the proof is complete. □

2.1 Weierstrass representation

In the period 1860-70, Enneper and Weierstrass obtained representation formulas for minimal surfaces in $\mathbb{R}^3$ by using curvature lines as parameter lines. Their formulae have become fundamental in the study of orientable minimal surfaces (for nonorientable minimal surfaces there are similar formulations, although we will not describe them here). The reader can find a detailed explanation of the Weierstrass representation in treatises on minimal surfaces by Hildebrandt et al. [8], Nitsche [35] and Osserman [36]. The starting point is the well-known formula

$$\Delta X = 2\, H\, N,$$

valid for an isometric immersion $X = (x_1, x_2, x_3)\colon M \to \mathbb{R}^3$ of a Riemannian surface into Euclidean space, where N is the Gauss map, H is the mean curvature and $\Delta X = (\Delta x_1, \Delta x_2, \Delta x_3)$ is the Laplacian of the immersion. In particular, minimality of M is equivalent to the harmonicity of the coordinate functions x_j, $j = 1, 2, 3$. In the sequel, it is worth considering M as a Riemann surface. We will also denote by $i = \sqrt{-1}$ and Re, Im will stand for real and imaginary parts.

We denote by x_j^* the harmonic conjugate of x_j, which is locally well-defined up to additive constants. Thus,

$$\phi_j := dx_j + i\, dx_j^*,$$

is a holomorphic 1-form, globally defined on M. If we choose a base point $p_0 \in M$, then the equality

$$X(p) = X(p_0) + \operatorname{Re} \int_{p_0}^{p} (\phi_1, \phi_2, \phi_3), \quad p \in M, \tag{4}$$

recovers the initial minimal immersion, where integration in (4) does not depend on the path in M joining p_0 to p.

The information encoded by ϕ_j, $j = 1, 2, 3$, can be expressed with only two pieces of data (this follows from the relation that $\sum_{j=1}^{3} \phi_j^2 = 0$); for instance, the meromorphic function $g = \frac{\phi_3}{\phi_1 - i\phi_2}$ together with ϕ_3 produce the other two 1-forms by means of the formulas

$$\phi_1 = \frac{1}{2}\left(\frac{1}{g} - g\right)\phi_3, \quad \phi_2 = \frac{i}{2}\left(\frac{1}{g} + g\right)\phi_3, \tag{5}$$

with the added bonus that g is the stereographic projection of the Gauss map N from the north pole, i.e.,

$$N = \left(2\,\frac{\mathrm{Re}(g)}{1+|g|^2}, 2\,\frac{\mathrm{Im}(g)}{1+|g|^2}, \frac{|g|^2-1}{1+|g|^2}\right).$$

We finish this preliminaries section with the statement of the celebrated Schwarz reflection principle that will be useful later. In 1894, H. A. Schwarz adapted his reflection principle for real-valued harmonic functions in open sets of the plane to obtain the following result for minimal surfaces. The classical proof of this principle can be found in Lemma 7.3 of [36], and a different proof, based on the so-called Björling problem, can be found in §3.4 of [8].

Lemma 2.2 (Schwarz)**.** *Any straight line segment (resp. planar geodesic) in a minimal surface is an axis of a* 180°*-rotational symmetry (resp. a reflective symmetry in the plane containing the geodesic) of the surface.*

3 Enneper's reduction of the classification problem to foliations by circles in parallel planes

We will say that a surface $M \subset \mathbb{R}^3$ is foliated by circles if it can be parameterized as

$$X(u,v) = c(u) + r(u)\left(\cos v\,\mathbf{v}_1(u) + \sin v\,\mathbf{v}_2(u)\right), \quad u_0 < u < u_1,\ 0 \le v < 2\pi, \tag{6}$$

where $c\colon (u_0, u_1) \to \mathbb{R}^3$ is a curve that parameterizes the centers of the circles in the foliation, and $r\colon (u_0, u_1) \to (0, \infty)$ is the radius of the foliating circle. Let $\mathbf{v}_1(u)$ and $\mathbf{v}_2(u)$ be an orthonormal basis of the linear subspace associated to the affine plane that contains the foliating circle. The purpose of this section is to prove Enneper's reduction.

Proposition 3.1 (Enneper)**.** *If a minimal surface $M \subset \mathbb{R}^3$ is foliated by circles, then these circles are contained in parallel planes.*

Proof. Let $\{\mathcal{C}_u \mid u \in (u_0, u_1)\}$ be the smooth, 1-parameter family of circles that foliate M. Let $t\colon (u_0, u_1) \to \mathbb{S}^2(1)$ be the unit normal vector to the plane that contains $\mathcal{C}_u$. It suffices to show that $t(u)$ is constant. Arguing by contradiction,

assume that t is not constant. After possibly restricting to a subinterval, we can suppose that $t'(u) \neq 0$ for all $u \in (u_0, u_1)$. Take a curve $\gamma : (u_0, u_1) \to \mathbb{R}^3$ with $\gamma'(u) = t(u)$, for all $u \in (u_0, u_1)$. The condition that $t'(u)$ vanishes nowhere implies that the curvature function $\kappa(u)$ of γ is everywhere positive. Let $n(u)$, $b(u)$ be the normal and binormal (unit) vectors to γ, i.e., $\{t, n, b\}$ is the Frenet dihedron of γ, and let τ be the torsion of γ. The surface M can be written as in (6) with $\mathbf{v}_1 = n$ and $\mathbf{v}_2 = b$. Our purpose is to express the minimality condition $H = 0$ in terms of this parameterization. To do this, denote by

$$E = |X_u|^2, \qquad F = \langle X_u, X_v \rangle, \qquad G = |X_v|^2,$$
$$e = \tfrac{\det(X_u, X_v, X_{uu})}{|X_u \wedge X_v|}, \quad f = \tfrac{\det(X_u, X_v, X_{uv})}{|X_u \wedge X_v|}, \quad g = \tfrac{\det(X_u, X_v, X_{vv})}{|X_u \wedge X_v|}$$

the coefficients of the first and second fundamental forms of M in the parameterization X.

If (α, β, δ) corresponds to the coordinates of the velocity vector c' of the curve of centers $c(u)$ with respect to the orthonormal basis $\{t, n, b\}$, then a straightforward computation that only uses the Frenet equations for γ leads to

$$\begin{aligned} e\,G - 2\,f\,F + E\,g = \tfrac{1}{|X_u \wedge X_v|}\,(a_1\,\cos(3\,v) + a_2\,\sin(3\,v) + \\ a_3\,\cos(2\,v) + a_4\,\sin(2\,v) + a_5\,\cos v + a_6\,\sin v + a_7)\,, \end{aligned}$$

where the functions a_j, $j = 1, \ldots, 7$ depend only on the parameter u and are given in terms of the radius $r(u)$ of $\mathcal{C}_u$ and the curvature $\kappa(u)$ and torsion $\tau(u)$ of γ by

$$\begin{aligned} a_1 &= -\tfrac{1}{2} r^3\,\kappa\,\left(\beta^2 - \delta^2 + r^2\,\kappa^2\right), \\ a_2 &= -r^3\,\beta\,\delta\,\kappa, \\ a_3 &= \tfrac{r^3}{2}\,\left(-6\,\beta\,\kappa\,r' + r\,\left(5\,\alpha\,\kappa^2 + \kappa\,\beta' - \beta\,\kappa'\right)\right), \\ a_4 &= \tfrac{r^3}{2}\,\left(r\,\kappa\,\delta' - \delta\,\left(6\,\kappa\,r' + r\,\kappa'\right)\right), \\ a_5 &= -\tfrac{r^2}{2}\,\left(3\,r^3\,\kappa^3 - 4\,\alpha\,\beta\,r' + r\,\left(8\,\alpha^2\,\kappa + 3\,\beta^2\,\kappa + 3\,\kappa\,\left(\delta^2 + 2\,(r')^2\right) - \right.\right. \\ &\qquad \left.\left. 2\,\beta\,\alpha' + 2\,\alpha\,\left(\delta\,\tau + \beta'\right)\right) + 2\,r^2\,\left(r'\,\kappa' - \kappa\,r''\right)\right), \\ a_6 &= r^2\,\left(2\,\alpha\,\delta\,r' + r^2\,\kappa\,\tau\,r' + r\,\left(\delta\,\alpha' + \alpha\,\left(\beta\,\tau - \delta'\right)\right)\right), \\ a_7 &= \tfrac{r^2}{2}\,\left(2\,\alpha^3 + r\,\left(2\,r'\,\left(-2\,\beta\,\kappa + \alpha'\right) + r\,\left(\kappa\,\left(2\,\delta\,\tau + \beta'\right) - \beta\,\kappa'\right)\right) + \right. \\ &\qquad \left. \alpha\,\left(2\,\beta^2 + 2\,\delta^2 + 5\,r^2\,\kappa^2 + 2\,(r')^2 - 2\,r\,r''\right)\right). \end{aligned}$$

As the functions in $\{\cos(n\,v), \sin((n+1)\,v) \mid n \in \mathbb{N} \cup \{0\}\}$ are linearly independent, then the condition $H = 0$ is equivalent to $a_j = 0$, for each $j = 1, \ldots, 7$. Since $r > 0$ and $\kappa > 0$, then the conditions $a_1 = a_2 = 0$ above imply that $\beta = 0$ and $\delta^2 = r^2\kappa^2$. Plugging this into $a_4 = 0$, we get $5r\,r'\,\kappa^2 = 0$, from where $r' = 0$. Substituting this into $a_3 = 0$ we get $5r\,\alpha\,\kappa^2 = 0$, hence $\alpha = 0$. Finally, plugging $\alpha = \beta = r' = 0$ and $\delta^2 = r^2\kappa^2$ into $a_5 = 0$, we deduce that $-3r^5\kappa^3 = 0$, which is a contradiction. This contradiction shows that $t(u)$ is constant and the proposition is proved. □

4 The argument by Riemann

In this section we explain the classification by Riemann of the minimal surfaces in $\mathbb{R}^3$ that are foliated by circles. By Proposition 3.1, we can assume that the foliating circles of our minimal surface $M \subset \mathbb{R}^3$ are contained in parallel planes, which after a rotation we will assumed to be horizontal. We will take the height z of the plane as a parameter of the foliation, and denote by $(\alpha(z), z) = (\alpha_1(z), \alpha_2(z), z)$ the center of the circle $M \cap \{x_3 = z\}$ and $r(z) > 0$ its radius; here we are using the identification $\mathbb{R}^3 = \mathbb{R}^2 \times \mathbb{R}$. The functions α_1, α_2, r are assumed to be of class C^2 in an interval $(z_0, z_1) \subset \mathbb{R}$.

Consider the function $F : \mathbb{R}^2 \times (z_0, z_1) \to \mathbb{R}$ given by

$$F(x, z) = |x - \alpha(z)|^2 - r(z)^2, \tag{7}$$

where $x = (x_1, x_2) \in \mathbb{R}^2$. So, $M \subset F^{-1}(\{0\})$ and thus, Lemma 2.1 gives that M is minimal if and only if

$$F_z^2 + |x - \alpha|^2 (2 + F_{zz}) + 2\langle x - \alpha, \alpha' \rangle F_z = 0 \quad \text{in } M.$$

As $|x-\alpha|^2 = r^2$ in M and $2\langle x-\alpha, \alpha' \rangle = -\left(|x - \alpha|^2\right)_z = -(F+r^2)_z = -F_z - (r^2)'$, then the minimality of M can be written as

$$2r^2 + r^2 F_{zz} - (r^2)' F_z = 0. \tag{8}$$

The argument amounts to integrating (8). First we divide by r^4,

$$0 = \frac{2}{r^2} + \frac{r^2 F_{zz} - (r^2)' F_z}{r^4} = \frac{2}{r^2} + \left(\frac{F_z}{r^2}\right)_z,$$

and then we integrate with respect to z, obtaining

$$f(x) = 2 \int^z \frac{du}{r(u)^2} + \frac{F_z(x, z)}{r(z)^2}, \tag{9}$$

for a certain function of x. On the other hand, (7) implies that

$$\frac{\partial}{\partial x_j}\left(\frac{F_z}{r^2}\right) = -\frac{2\alpha_j'}{r^2},$$

which is a function depending only on z, for each $j = 1, 2$. Therefore, for z fixed, the function $x \mapsto \frac{F_z}{r^2}$ must be affine. As $\int^z \frac{du}{r(u)^2}$ only depends on z, we conclude from (9) that $f(x)$ is also an affine function of x, i.e.,

$$2 \int^z \frac{du}{r(u)^2} + \frac{F_z(x, z)}{r(z)^2} = 2\langle a, x \rangle + c \tag{10}$$

for certain $a = (a_1, a_2) \in \mathbb{R}^2$, $c \in \mathbb{R}$. Taking derivatives in (10) with respect to x_j, we get $\alpha_j'(z) = -a_j r^2(z)$; hence

$$\alpha(z) = -m(z)\, a \quad \text{where } m(z) = \int^z r(u)^2\, du.$$

These formulas determine the center of the circle $M \cap \{x_3 = z\}$ up to a horizontal translation that is independent of the height.

In order to determine the radius of the circle $M \cap \{x_3 = z\}$ as a function of z, we come back to equation (8). Since $F_z = -2\langle x - \alpha, \alpha' \rangle - (r^2)'$, then $F_{zz} = 2|\alpha'|^2 - 2\langle x - \alpha, \alpha'' \rangle - (r^2)''$. Plugging $\alpha' = -r^2\, a$ into these two expressions, and this one into (8), we deduce that the minimality of M can be rewritten as

$$2|a|^2 r^6 + ((r^2)')^2 + r^2(2 - (r^2)'') = 0, \tag{11}$$

which is an ordinary differential equation in the function $q(z) = r(z)^2$. Solving this ODE is straightforward: first note that

$$\left(\frac{(q')^2}{q^2}\right)' = \frac{2q'}{q^3}\left[-(q')^2 + qq''\right] \overset{(11)}{=} \frac{2q'}{q^3}\left(2|a|^2 q^3 + 2q\right) = 4\left(|a|^2 q' + \frac{q'}{q^2}\right).$$

Hence integrating with respect to z we have

$$\frac{(q')^2}{q^2} = 4\left(|a|^2 q - \frac{1}{q}\right) + 4\lambda, \tag{12}$$

for certain $\lambda \in \mathbb{R}$. In particular, the right-hand side of (12) must be nonnegative. Solving for $q'(z)$ we have

$$q' = \frac{dq}{dz} = 2\sqrt{|a|^2 q^3 - q + \lambda q^2};$$

hence the height differential of M is

$$dz = \frac{1}{2}\frac{dq}{\sqrt{|a|^2 q^3 - q + \lambda q^2}},$$

where $q = r^2$. Viewing q as a real variable, the third coordinate function of M can be expressed as

$$z(q) = \frac{1}{2}\int^q \frac{du}{\sqrt{|a|^2 u^3 - u + \lambda u^2}}. \tag{13}$$

To obtain the first two coordinate functions of M, recall that $M \cap \{x_3 = z\}$ is a circle centered at (α, z) with radius r. This means that besides the variable q that gives the height $z(q)$, we need another real variable to parameterize the circle centered at (α, z) with radius r:

$$x(q, v) = \alpha(z(q)) + \sqrt{q}e^{iv} = -m(z(q))\, a + \sqrt{q}e^{iv} = -\int^{z(q)} q(z)\, dz \cdot a + \sqrt{q}e^{iv}$$

$$= -\int^q q\frac{dz}{dq}\, dq \cdot a + \sqrt{q}e^{iv} = -\frac{1}{2}\int^q \frac{u\, du}{\sqrt{|a|^2 u^3 - u + \lambda u^2}} \cdot a + \sqrt{q}e^{iv},$$

where $0 \le v < 2\pi$. In summary, we have obtained the following parameterization $X = (x_1, x_2, z) = (x_1 + ix_2, z)$ of M:

$$X(q, v) = f(q)(a, 0) + \sqrt{q}(e^{iv}, 0) + (0, z(q)), \tag{14}$$

where $f(q) = -\frac{1}{2}\int^q \frac{u\,du}{\sqrt{|a|^2u^3 - u + \lambda u^2}}$ and $z(q)$ is given by (13).

The surfaces in (14) come in a 3-parameter family depending on the values of a_1, a_2, λ. Nevertheless, two of these parameters correspond to rotations and homotheties of the same geometric surface, and so there is only one genuine geometric parameter.

Next we will analyze further the surfaces in the family (14), in order to understand their shape and other properties. First observe that the first term in the last expression of $X(q,v)$ parameterizes the center of the circle $M \cap \{x_3 = z(q)\}$ as if it were placed at height zero, the second term parameterizes the circle itself (q is positive as $q(z) = r(z)^2$), and the third one places the circle at height $z(q)$. To study the shape of the surface, we will analyze for which values of $q > 0$ the radicand $|a|^2q^3 - q + \lambda q^2$ is nonnegative (this is a necessary condition, see (12)). This indicates that the range of q is of the form $[q_1, +\infty)$ for certain $q_1 > 0$. Also, the positivity of the integrand in (13) implies that $z(q)$ is increasing. Since choosing a starting value of q for the integral (13) amounts to vertically translating the surface, we can choose this starting value as q_1, which geometrically means:

> *We normalize M so that the circle of minimum radius in M is at height zero, and M is a subset of the half-space $\{(x_1, x_2, x_3) \mid x_3 \geq 0\}$.*

This translated surface will have a lower boundary component being a circle (or in the limit case a straight line) contained in the plane $\{z = 0\}$ (in particular, M is not complete). If we choose the negative branch of the square root when solving for $q'(z)$ after (12), we will obtain another surface M' contained in the half-space $\{x_3 \leq 0\}$ with the same boundary as M in $\{x_3 = 0\}$. The union of M with M' is again a smooth minimal surface; this is because the tangent spaces to both M, M' coincide along the common boundary. Nevertheless, $M \cup M'$ might fail to be complete; we will obtain more information about this issue of completeness when discussing the value of a.

Analogously, picking a starting value of q for the integral in (14) that gives f, corresponds to translating horizontally the center of the circle $M \cap \{x_3 = z(q)\}$ by a vector independent of q, or equivalently, translating M horizontally in $\mathbb{R}^3$. Thus, we can normalize this starting value of q for the integral in (14) to be the same q_1 as before. This means that we may assume:

> *The circle of minimum radius in M has its center at the origin of $\mathbb{R}^3$.*

We next discuss cases depending on whether or not a vanishes.

Case I: $a = (0,0)$ gives the catenoid.

In this case, (14) reads $X(q,v) = \sqrt{q}(e^{iv}, 0) + (0, z(q))$, where $z(q) = \frac{1}{2}\int_{q_1}^q \cdot \frac{du}{\sqrt{-u+\lambda u^2}}du$. In particular, M is a surface of revolution around the z-axis, so M is a half-catenoid with neck circle at height zero. In order to determine q_1, observe that λ is positive as follows from (12)), and that the function $u \mapsto -u + \lambda u^2$ is nonnegative in $(-\infty, 0] \cup [\frac{1}{\lambda}, \infty)$. Therefore, we must take $q_1 = \frac{1}{\lambda}$. Furthermore,

the integral that defines $z(q)$ can be explicitly solved:

$$z(q) = \frac{1}{2}\int_{1/\lambda}^{q} \frac{du}{\sqrt{-u+\lambda u^2}} du = \frac{1}{\lambda}\,\mathrm{arg\,sinh}\,\sqrt{-1+q\lambda},$$

which gives the following parameterization of M:

$$X(q,v) = \left(\sqrt{q}e^{iv}, \frac{1}{\lambda}\,\mathrm{arg\,sinh}\,\sqrt{-1+q\lambda}\right). \tag{15}$$

In this case, the surface $M' \subset \{x_3 \leq 0\}$ defined by the negative branch of the square root when solving for $q'(z)$ in (12) is the lower half of the same catenoid of which M is the upper part. In particular, $M \cup M'$ is complete.

Case II: $a \neq (0,0)$ gives the Riemann minimal examples.

As f, z depend on $|a|^2$ but not on $a = (a_1, a_2)$, then a rotation of $a \equiv a_1 + ia_2$ in $\mathbb{R}^2 \equiv \mathbb{C}$ around the origin by angle θ will leave f and z invariant. By (14), the center of the circle $M \cap \{x_3 = z(q)\}$ will be also rotated by the same angle θ around the x_3-axis, while the second and third terms in (14) will remain the same. This says that rotating a in $\mathbb{C}$ corresponds to rotating M in $\mathbb{R}^3$ around the x_3-axis, so without lost of generality we can assume that $a \equiv (a,0) \in \mathbb{R}^2$ with $a > 0$.

The radicand of equation (13) is now expressed by $q(a^2q^2 - 1 + \lambda q)$, hence $a^2q^2 - 1 + \lambda q \geq 0$. This occurs for $q \in \left[\frac{1}{2a^2}(-\lambda - \sqrt{4a^2+\lambda^2}), 0\right] \cup [q_1, \infty)$, where

$$q_1 = \frac{1}{2a^2}(-\lambda + \sqrt{4a^2+\lambda^2}).$$

As $q > 0$, then the correct range is $q \in [q_1, \infty)$. Now fix the starting integration values for $z(q), f(q)$ at q_1, and denote by $z_{a,\lambda}, f_{a,\lambda}$ the functions given by (13), (14), respectively. A straightforward change of variables shows that

$$\sqrt{a}z_{a,\lambda}(q) = z_{1,\lambda/a}(aq), \qquad a^{3/2}f_{a,\lambda}(q) = f_{1,\lambda/a}(aq).$$

Thus, the minimal immersions $X_{a,\lambda}, X_{1,\lambda/a}$ are related by a homothety of ratio $\sqrt{a}$:

$$\sqrt{a}X_{a,\lambda}(q,v) = X_{1,\lambda/a}(aq,v).$$

Therefore, we can assume $a = 1$, i.e., our surfaces only depend on the real parameter λ:

$$X_\lambda(q,v) = f_\lambda(q)(1,0) + \sqrt{q}(e^{iv},0) + (0, z_\lambda(q)), \tag{16}$$

where

$$f_\lambda(q) = -\frac{1}{2}\int_{q_1}^{q} \frac{u\,du}{\sqrt{u^3-u+\lambda u^2}}, \quad z_\lambda(q) = \frac{1}{2}\int_{q_1}^{q} \frac{u\,du}{\sqrt{u^3-u+\lambda u^2}} \quad \text{and}$$

$$q_1 = q_1(\lambda) = \frac{1}{2}\left(-\lambda + \sqrt{4+\lambda^2}\right).$$

Calling $M_\lambda = X_\lambda([q_1,\infty)\times[0,2\pi))$, the center of the circle $M_\lambda \cap \{x_3 = z_\lambda(q)\}$ lies en the plane $\Pi \equiv \{x_2 = 0\}$, which implies that M_λ is symmetric with respect to Π.

The increasing function $q \mapsto z_\lambda(q)$, $q \in [q_1, \infty)$, is bounded because $\int^q \frac{du}{\sqrt{u^3}}$ has limit zero as $q \to \infty$. This means that M_λ lies in a slab of the form

$$S(0,\zeta) = \{(x_1, x_2, z) \in \mathbb{R}^3 \mid 1 \le z \le \zeta\},$$

where $\zeta = \zeta(\lambda) = \lim_{q\to\infty} z_\lambda(q) > 0$.

We next analyze $M_\lambda \cap \{x_3 = \zeta\}$. As M_λ is symmetric with respect to Π, given $q \in [q_1, \infty[$, the circle $M_\lambda \cap \{x_3 = z(q)\}$ intersects Π at two antipodal points $A_+(q), A_-(q)$ that are obtained by imposing the condition $\sin v = 0$ in (16), i.e.,

$$A_\pm(q) = \left(-\frac{1}{2}\int_{q_1}^{q} \frac{u\,du}{\sqrt{u^3 - u + \lambda u^2}} \pm \sqrt{q}, z_\lambda(q) \right) \in (\mathbb{R} \times \{0\}) \times \mathbb{R} \subset \mathbb{C} \times \mathbb{R}.$$

Since q is not bounded, the first coordinate of $A_-(q)$ tends to $-\infty$ as $q \to \infty$, that is to say, when we approach the upper boundary plane $\{x_3 = \zeta\}$ of the slab $S(0,\zeta)$. On the contrary, the first coordinate of $A_+(q)$ tends to a finite limit as $q \to \infty$, because for sufficiently large values of q we have

$$\left(-\frac{1}{2}\int_{q_1}^{q} \frac{u\,du}{\sqrt{u^3 - u + \lambda u^2}} + \sqrt{q} \right) \approx \left(\text{constant}(\lambda) - \frac{1}{2}\int_{q_1}^{q} \frac{du}{\sqrt{u}} + \sqrt{q} \right) = \text{constant}(\lambda).$$

Therefore, $A_+(q)$ converges as $q \to \infty$ to a point $A \in \{x_3 = \zeta\} \cap \Pi$. This proves that $M_\lambda \cap \{x_3 = \zeta\} \neq \emptyset$. As $M_\lambda \cap \{x_3 = \zeta\}$ cannot be compact (because $A_-(q)$ diverges in $\mathbb{R}^3$ as $q \to \infty$), we deduce that $M_\lambda \cap \{x_3 = \zeta\}$ is a noncompact limit of circles symmetric with respect to Π, hence it is a straight line r orthogonal to Π and passing through A.

As the boundary of M_λ consists of a circle in $\{x_3 = 0\}$ and a straight line r in $\{x_3 = \zeta\}$, then the Schwarz reflection principle (Lemma 2.2) implies that $M \cup \mathrm{Rot}_r(M)$ is a minimal surface, where Rot_r denotes the 180°-rotation around r. Clearly, $M \cup \mathrm{Rot}_r(M) \subset S(0, 2\,\zeta)$ has two horizontal boundary circles of the same radius. The same behavior holds if we choose the negative branch of the square root when solving (12) for $q'(z)$, but now for a slab of the type $S(-\zeta, 0)$. This means that we can rotate the surface by 180° around the straight line $r' = \{-p \mid p \in r\} \subset \{x_3 = -\zeta\}$, obtaining a minimal surface that lies in $S(-4\,\zeta, 2\,\zeta)$, whose boundary consists of two circles of the same radius in the boundary planes of this slab and such that the surface contains in its interior three parallel straight lines at heights ζ, $-\zeta$, $-3\,\zeta$, all orthogonal to Π. Repeating this rotation-extension process indefinitely we produce a complete embedded minimal surface $R_\lambda \subset \mathbb{R}^3$ that contains parallel lines contained in the planes $\{x_3 = (2k+1)\zeta(\lambda)\}$ with $k \in \mathbb{Z}$ and orthogonal to Π. It is also clear that R_λ is invariant under the translation T_λ by the vector $2(A - B)$ (here $B = r' \cap \Pi$), obtained by the composition of two 180°-rotations in consecutive lines. This surface R_λ is what we call a *Riemann minimal example,* and it is foliated by circles and lines in parallel planes.

For each Riemann minimal example R_λ, the circles of minimum radius lie in the planes $\{x_3 = 2\,k\,\zeta\,(\lambda)\}$, $k \in \mathbb{Z}$, and this minimum radius is

$$\sqrt{q_1(\lambda)} = \sqrt{(-\lambda + \sqrt{4 + \lambda^2})/2}.$$

This function of $\lambda \in \mathbb{R}$ is one-to-one (with negative derivative), from where we conclude that

> *The Riemann minimal examples* $\{R_\lambda \mid \lambda \in \mathbb{R}\}$ *form a 1-parameter family of noncongruent surfaces.*

In Figure 1 we have represented the intersection of R_λ for $\lambda = 1$ with the symmetry plane Π. At each of the points A and B there passes a straight line contained in the surface and orthogonal to Π.

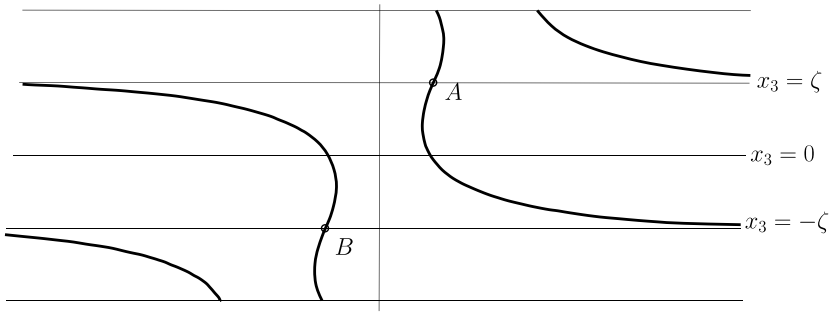

Figure 1: The intersection of R_λ with the symmetry plane $\Pi = \{x_2 = 0\}$. The translation of vector $2(A - B)$ leaves R_λ invariant.

Viewed as a complete surface in $\mathbb{R}^3$, each Riemann minimal example R_λ has the topology of an infinite cylinder punctured in an infinite discrete set of points, corresponding to its planar ends, and R_λ is invariant under a translation T_λ. Furthermore, quotient surface $\mathcal{R}_\lambda = R_\lambda/T_\lambda$ in the 3-dimensional flat Riemannian manifold $\mathbb{R}^3/T_\lambda$ is conformally diffeomorphic to a flat torus $\mathbb{T}$ punctured in two points. In addition, the Gauss map G of $\mathcal{R}_\lambda$ has degree two and has exactly two branch points. This means that G is a meromorphic function on the punctured torus that extends to a meromorphic function $\widehat{G}$ of degree two on $\mathbb{T}$ whose zeros and poles of order two occur at the two points corresponding to the planar ends of $\mathcal{R}_\lambda$ in $\mathbb{R}^3/T_\lambda$. It then follows from Riemann surface theory that the degree-two meromorphic function $\widehat{G}$ is a complex multiple of the Weierstrass $\mathcal{P}$-function on the underlying elliptic curve $\mathbb{T}$. Furthermore, the vertical plane of symmetry and the rotational symmetry around either of the two lines on the quotient surface $\mathcal{R}_\lambda$ imply that $\mathbb{T}$ is conformally $\mathbb{C}/\Lambda$ where Λ is a rectangular lattice.

4.1 Graphics representation of the Riemann minimal examples

With the parameterizations of the Riemann minimal examples obtained in the preceding section we can represent these surfaces with the help of the Mathematica graphing package. Nevertheless, we will not use the parameterization in (16), mainly because the parameter q diverges when producing the straight lines

contained in R_λ; instead, we will use a conformal parameterization given by the Weierstrass representation.

Recall that $\mathcal{R}_\lambda = R_\lambda/T_\lambda$ is a twice punctured torus, and that its Gauss map (which can be regarded as a holomorphic function on $\mathcal{R}_\lambda$, see Section 2.1) has degree two on the compactification. In particular, the compactification of $\mathcal{R}_\lambda$ is conformally equivalent to the following algebraic curve:

$$\overline{M}_\sigma = \left\{(z,w) \in \overline{\mathbb{C}} \times \overline{\mathbb{C}} \mid w^2 = z(z-1)(z+\sigma)\right\},$$

where $\sigma \in \mathbb{C} - \{0,1\}$ depends on λ in some way to be determined later, and we can moreover choose the degree-two function z on $\overline{M}_\sigma$ so that meromorphic extension of the Gauss map of $\mathcal{R}_\lambda$ to $\overline{M}_\sigma$ is $g^\sigma(z,w) = \rho\, z$, for a certain constant $\rho = \rho(\sigma) \in \mathbb{C}^*$. It is worth mentioning that the way one endows $\overline{M}_\sigma$ with a complex structure is also due to Riemann, when studying multivalued functions on the complex plane (in this case, $z \mapsto \sqrt{z(z-1)(z+\sigma)}$).

Since the third coordinate function of R_λ is harmonic and extends analytically through the planar ends (because it is bounded in a neighborhood of each end), its complex differential $dx_3 + i\, dx_3^* = \phi_3^\sigma$ is a holomorphic 1-form on the torus $\overline{M}_\sigma$ (without zeros). As the linear space of holomorphic 1-forms on a torus has complex dimension 1, then we deduce that $\phi_3^\sigma \equiv \mu \frac{dz}{w}$ for some $\mu \in \mathbb{C}^*$ also to be determined. Clearly, after possibly applying a homothety to R_λ, we can assume that $|\mu| = 1$.

4.1.1 Symmetries of the surface

Recall that each surface R_λ is invariant under certain rigid motions of $\mathbb{R}^3$, which therefore induce intrinsic isometries of the surface. These intrinsic isometries are in particular conformal diffeomorphisms of the algebraic curve $\overline{M}_\sigma$, that might be holomorphic or anti-holomorphic depending on whether or not they preserve or invert the orientation of the surface. These symmetries will be useful in determining the constants that appeared in the above two paragraphs.

First consider the orientation-preserving isometry of R_λ given by 180°-rotation about a straight line parallel to the x_2-axis, that intersects R_λ orthogonally at two points lying in a horizontal circle of minimum radius (these points would be represented by the mid point of the segment $\overline{AB}$ in Figure 1). This symmetry induces an order-two biholomorphism S_1 of $\overline{M}_\sigma$, that acts on g^σ, ϕ_3^σ in the following way:

$$g^\sigma \circ S_1 = -1/g^\sigma, \qquad S_1^* \phi_3^\sigma = -\phi_3^\sigma.$$

As S_1 interchanges the branch values of g, we deduce that $\rho = \frac{1}{\sqrt{\sigma}}$ and $S_1(z,w) = (-\frac{\sigma}{z}, -\sigma\frac{w}{z^2})$.

Another isometry of R_λ is the 180°-rotation about a straight line r parallel to the x_2-axis and contained in the surface. As this symmetry reverses orientation of R_λ, then it induces an order-two anti-holomorphic diffeomorphism S_2 of $\overline{M}_\sigma$, that acts on g^σ, ϕ_3^σ as

$$g^\sigma \circ S_2 = \overline{g^\sigma} \qquad S_2^* \phi_3^\sigma = -\overline{\phi_3^\sigma}.$$

S_2 fixes the branch points of g^σ (one of them lies in r), from where we get $\sigma \in \mathbb{R}$, $\mu \in \{\pm 1, \pm i\}$ and $S_2(z,w) = (\overline{z}, \pm\overline{w})$. Furthermore, the unit normal vector to R_λ along r takes values in $\mathbb{S}^1(1) \cap \{x_2 = 0\}$, which implies that $g^\sigma(1,0) \in \mathbb{R}$, and so, $\sigma > 0$.

The following argument shows that we can assume that $\mu = 1$. Consider the Weierstrass data $\big(\overline{M}_\sigma,\ g^\sigma,\ \phi_3^\sigma\big)$, and the biholomorphism $\Sigma\colon \overline{M}_{1/\sigma} \to \overline{M}_\sigma$ given by $\Sigma(z,w) = (-\sigma\, z, i\, \sigma^{3/2}\, w)$. Then, we have that

$$g^\sigma \circ \Sigma = -g^{1/\sigma}, \quad \Sigma^* \phi_3^\sigma = \frac{i}{\sqrt{\sigma}} \phi_3^{1/\sigma}.$$

The change of variable via Σ gives

$$\int_{\Sigma(P_0)}^{\Sigma(P)} \frac{i}{\sqrt{\sigma}} \phi_3^{1/\sigma} = \int_{P_0}^{P} \phi_3^\sigma,$$

and similar equations hold for the other two components $\phi_1^{1/\sigma}, \phi_2^{1/\sigma}$ of the Weierstrass form (see (5)). This implies that we can assume after a rigid motion and homothety, that $\mu = 1$ and that the isometry S_2 is

$$S_2(z,w) = (\overline{z}, -\overline{w}).$$

Finally, the reflective symmetry of R_λ with respect to the plane $\{x_2 = 0\}$ induces an anti-holomorphic involution S_3 of $\overline{M}_\sigma$ which fixes the branch points of g^σ (including the zeros and poles $(0,0), (\infty,\infty)$ of g, which correspond to the ends of $\mathcal{R}_\lambda$), and that preserves the third coordinate function. It is then clear that this transformation has the form $S_3(z,w) = (\overline{z}, \overline{w})$.

4.1.2 The period problem

We next check that the Weierstrass data $\big(\overline{M}_\sigma,\ g^\sigma,\ \phi_3^\sigma\big)$ produces a minimal surface in $\mathbb{R}^3$, invariant under a translation vector. A homology basis of the algebraic curve $\overline{M}_\sigma$ is $\mathcal{B} = \{\gamma_1, \gamma_2\}$, where these closed curves are the liftings to $\overline{M}_\sigma$ through the z-projection of the curves in the complex plane represented in Figure 2.

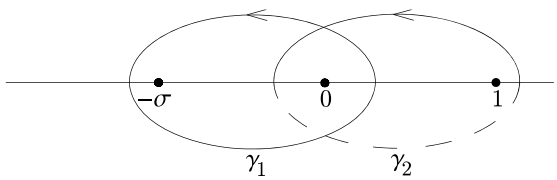

Figure 2: The curves γ_1 and γ_2 in the z-complex plane.

The action of the symmetries S_j, $j = 1,2,3$, on the basis $\mathcal{B}$ and on the Weierstrass data implies that

$$\mathrm{Re} \int_{\gamma_1} (\phi_1^\sigma, \phi_2^\sigma, \phi_3^\sigma) = 0, \qquad \mathrm{Re} \int_{\gamma_2} (\phi_1^\sigma, \phi_2^\sigma, \phi_3^\sigma) \in \{x_2 = 0\}.$$

In particular, the Weierstrass data $\left(\overline{M}_\sigma,\ g^\sigma,\ \phi_3^\sigma\right)$ gives rise to a well-defined minimal immersion on the cyclic covering of $\overline{M}_\sigma - \{(0,0),(\infty,\infty)\}$ associated to the subgroup of the fundamental group of $\overline{M}_\sigma$ generated by γ_2. We will call $M_\sigma \subset \mathbb{R}^3$ to the image of this immersion; we will prove in Section 4.2 that M_σ is one of the Riemann minimal examples R_λ obtained in Section 4.

For the moment, we will content ourselves with finding a simply connected domain of M_σ bordered by symmetry lines (planar geodesics or straight lines). The reason for this is that the package Mathematica works with parameterizations defined in domains of the plane, which once represented graphically, can be replicated in space by means of the Schwarz reflection principles; we will call such a simply connected domain of M_σ a *fundamental piece.* Having in mind how the isometries S_2 and S_3 act on the z-complex plane, it is clear that we can reduce ourselves to representing graphically the domain of M_σ that corresponds to moving z in the upper half-plane. Using the symmetry S_1 we can reduce even further this domain, to the set $\left\{z \in \mathbb{C} \mid \left|z - \frac{1-\sigma}{2}\right| \leq \frac{1+\sigma}{2},\ \mathrm{Im}(z) \geq 0\right\}$. As the point $(z,w) = (0,0)$ corresponds to an end of the minimal surface M_σ, we will remove a small neighborhood of in the z-plane centered at the origin. In this way we get a planar domain Ω_σ as in Figure 3.

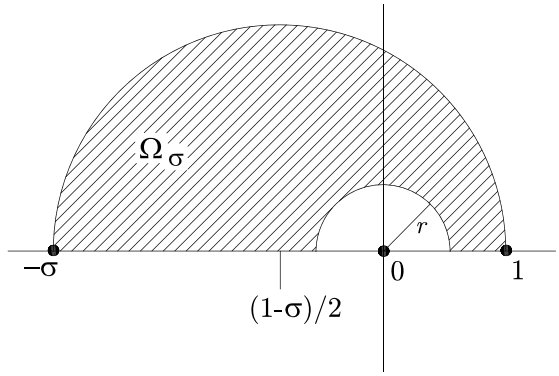

Figure 3: The domain Ω_σ.

The above arguments lead to the conformal parameterization $X^\sigma = (x_1^\sigma, x_2^\sigma, x_3^\sigma) : \Omega_\sigma \to \mathbb{R}^3$ given by

$$x_1^\sigma(z) = \mathrm{Re}\left(\int_1^z \frac{1}{2}\left(\frac{\sqrt{\sigma}}{u} - \frac{u}{\sqrt{\sigma}}\right)\frac{d\,u}{\sqrt{u(u-1)(u+\sigma)}}\right),$$

$$x_2^\sigma(z) = \mathrm{Re}\left(\int_1^z \frac{i}{2}\left(\frac{\sqrt{\sigma}}{u} + \frac{u}{\sqrt{\sigma}}\right)\frac{d\,u}{\sqrt{u(u-1)(u+\sigma)}}\right),$$

$$x_3^\sigma(z) = \mathrm{Re}\left(\int_1^z \frac{d\,u}{\sqrt{u(u-1)(u+\sigma)}}\right).$$

The following properties are easy to check from the symmetries of the Weierstrass

data:

(P1) The image through X^σ of the boundary segment $[-\sigma, 0] \cap \partial\Omega_\sigma$ corresponds to a planar geodesic of reflective symmetry of M_σ, contained in the plane $\{x_2 = 0\}$.

(P2) The image through X^σ of $[0, 1] \cap \partial\Omega_\sigma$ is a straight line segment contained in the surface and parallel to the x_2-axis.

(P3) The image through X^σ of the outer half-circle in $\partial\Omega_\sigma$ is a curve in M_σ which is invariant under the 180°-rotation around a straight line parallel to the x_2-axis, that passes through the fixed point $X^\sigma(i\sqrt{\sigma})$ of S_1.

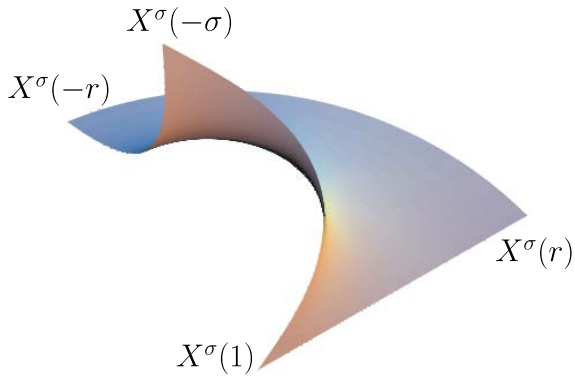

Figure 4: The fundamental piece for $\sigma = 1$.

After reflecting the fundamental piece $X^\sigma(\Omega_\sigma)$ across its boundary, we will obtain the complete minimal surface $M_\sigma \subset \mathbb{R}^3$.

4.2 Relationships between M_σ and R_λ: the Shiffman function

Each of the minimal surfaces $M_\sigma \subset \mathbb{R}^3$, $\sigma > 0$, constructed in the last section is topologically a cylinder punctured in an infinite discrete set of points, and M_σ has no points with horizontal tangent plane. For a minimal surface with these conditions, M. Shiffman introduced in 1956 a function that expresses the variation of the curvature of planar sections of the surface. More precisely, around a point p of a minimal surface M with nonhorizontal tangent plane, one can always pick a local conformal coordinate $\xi = x + i\,y$ so that the height differential is $\phi_3 = d\,\xi$. The horizontal level curves $\{x_3 = c\} \cap M$ near p are then parameterized as $\xi_c(y) = c + i\,y$. If we call κ_c to the curvature of this level section as a planar curve, then one can check that

$$\kappa_c(y) = \left[\frac{|g|}{1 + |g|^2} \operatorname{Re}\left(\frac{g'}{g}\right) \right] |_{\xi = \xi_c(y)},$$

where g is the Gauss map of M in this local coordinate, see Section 2.1. The Shiffman function is defined as

$$S_M = \Lambda \frac{\partial \kappa_c}{\partial y},$$

where $\Lambda > 0$ is the smooth function so that the induced metric on M is $ds^2 = \Lambda^2 |d\xi|^2$. In particular, the vanishing of the Shiffman function is equivalent to the fact that M is foliated by arcs of circles or straight lines in horizontal planes. Therefore, a way to show that the surface M_σ defined in the last section coincides with one of the Riemann minimal examples R_λ is to verify that its Shiffman function vanishes identically.

A direct computation shows that

$$S_M = \operatorname{Im}\left[\frac{3}{2}\left(\frac{g'}{g}\right)^2 - \frac{g''}{g} - \frac{1}{1+|g|^2}\left(\frac{g'}{g}\right)^2\right], \tag{17}$$

For the surface M_σ, we have $g(z,w) = g^\sigma(z,w)\frac{z}{\sqrt{\sigma}}$ and $d\xi = \phi_3^\sigma = \frac{dz}{w} = \sqrt{\sigma}\frac{g'\,d\xi}{w}$; hence $w = \sqrt{\sigma} g'$ and thus $(g')^2 = g\,(\sqrt{\sigma}+g)\,(-1+\sqrt{\sigma}\,g)$. Taking derivatives of this expression we obtain $g'' = \frac{-\sqrt{\sigma}}{2} + \left(-1+\sqrt{\sigma}^2\right) g + \frac{3\sqrt{\sigma}\,g^2}{2}$. Plugging this in (17) we get

$$S_M = \operatorname{Im}\left[\frac{(\sigma-1)\left(|g|^2-1\right) - 4\sqrt{\sigma}\operatorname{Re}(g)}{2\left(1+|g|^2\right)}\right] = 0,$$

which implies that M_σ is one of the Riemann minimal examples R_λ, but which one?

We must look for an expression of $\sigma > 0$ in terms of $\lambda \in \mathbb{R}$ (or vice versa), so that the surfaces R_λ and M_σ are congruent. Since $g^\sigma(1,0) = 1/\sqrt{\sigma}$, $g^\sigma(-\sigma,0) = -\sqrt{\sigma}$, and we know that $X^\sigma(1,0)$, $X^\sigma(-\sigma,0)$ are points where straight lines contained in M_σ intersect the vertical plane of symmetry, the values of the stereographically projected Gauss map of the surface at these points will help us to find $\sigma(\lambda)$. Recall that with the parameterization $X_\lambda(q,v)$ of R_λ given in equation (16), these points are given by taking $v = 0$ and $q \to \infty$. Hence we must compute the limit as $q \to \infty$ of $\frac{N_1(q,0)}{1-N_3(q,0)}$, where $N = (N_1, N_2, N_3)$ is the Gauss map associated to X_λ. This limit is $\frac{2}{\lambda - \sqrt{\lambda^2+4}} < 0$, so we must impose it to coincide with $-\sqrt{\sigma}$. In other words,

$$\sigma = \left(\frac{2}{\sqrt{\lambda^2+4}-\lambda}\right)^2.$$

4.2.1 Parameterizing the surface with Mathematica

When using Mathematica, we must keep in mind that the germs of multivalued functions that appear in the integration of the Weierstrass representation are necessarily continuous. These choices of branches do not always coincide with the choices made by the program, but we do not want to bother the reader with

these technicalities. Thus, we directly write the three coordinate functions of the parameterization (already integrated) as follows:

$$\begin{aligned}
\texttt{x1}[\sigma_][\texttt{z_}] &:= \tfrac{1}{\sqrt{\sigma}}\left(\left(\sqrt{\tfrac{-1+z}{z}}\sqrt{z+\sigma}+\right.\right.\\
&\quad \tfrac{1}{\sqrt{1+\sigma}}\left(2\left((-1-\sigma)\texttt{EllipticE}\left[\texttt{ArcSin}\left[\sqrt{1+\tfrac{\texttt{z}}{\sigma}}\right],\tfrac{\sigma}{1+\sigma}\right]+\right.\right.\\
&\quad \left.\left.\left.\texttt{EllipticF}\left[\texttt{ArcSin}\left[\sqrt{1+\tfrac{\texttt{z}}{\sigma}}\right],\tfrac{\sigma}{1+\sigma}\right]\right)\right)\right)\\
\texttt{x2}[\sigma_][\texttt{z_}] &:= -\sqrt{\tfrac{-1+z}{-\sigma\, z}}\,\sqrt{\sigma+z}\\
\texttt{x3}[\sigma_][\texttt{z_}] &:= \tfrac{-2}{\sqrt{\sigma}}\texttt{EllipticF}\left[\texttt{ArcSin}\left[\tfrac{\sqrt{\sigma}}{\sqrt{\sigma+\texttt{z}}}\right],\tfrac{1+\sigma}{\sigma}\right]
\end{aligned}$$

We will translate the surface so that the point $v_0^\sigma = X^\sigma(1)$ equals the origin, defining the parameterization $\psi^\sigma(z) = X^\sigma(z) - v_0^\sigma$:

$$\begin{aligned}
\texttt{v0}[\sigma_] \quad &:= \left\{-2\,\texttt{Im}\left[\tfrac{1}{\sqrt{-(1+\sigma)\,\sigma}}\left((-1-\sigma)\ \texttt{EllipticE}\left[\texttt{ArcSin}\left[\sqrt{\tfrac{1+\sigma}{\sigma}}\right],\tfrac{\sigma}{1+\sigma}\right]+\right.\right.\right.\\
&\quad \left.\left.\left.\texttt{EllipticF}\left[\texttt{ArcSin}\left[\sqrt{\tfrac{1+\sigma}{\sigma}}\right],\tfrac{\sigma}{1+\sigma}\right]\right)\right],0,\\
&\quad -2\,\texttt{Re}\left[\tfrac{1}{\sqrt{\sigma}}\texttt{EllipticF}\left[\texttt{ArcSin}\left[\sqrt{\tfrac{\sigma}{1+\sigma}}\right],\tfrac{1+\sigma}{\sigma}\right]\right]\Big\}
\end{aligned}$$

$$\psi[\sigma\_][\texttt{z\_}] := \texttt{Re}[\{\texttt{x1}[\sigma][\texttt{z}],\texttt{x2}[\sigma][\texttt{z}],\texttt{x3}[\sigma][\texttt{z}]\}] - \texttt{v0}[\sigma]$$

In order to simplify our parameterization, we will use a Möbius transformation that maps the half-annulus $\{e \le |z| \le 1,\ \mathrm{Im}(z) \ge 0\}$, for certain $e \in (0,1)$, into the domain region Ω_σ; we will also use polar coordinates in the half-annulus:

$$\begin{aligned}
\texttt{f}[\texttt{z_},\texttt{a_},\texttt{e_}] := {} & (-\texttt{a}^2(1+\texttt{e}^2)(-1+\texttt{z}) - 2\texttt{a}(-3+\texttt{e}^2)\texttt{z} - (1+\texttt{e}^2)(1+\texttt{z}) +\\
& \texttt{Sqrt}[4(-1+\texttt{a})^2\texttt{e}^2 + (1+\texttt{a})^2(-1+\texttt{e}^2)^2](1+\texttt{a}(-1+\texttt{z})+\texttt{z}))\\
& (2\,\texttt{Sqrt}[4(-1+\texttt{a})^2\texttt{e}^2 + (1+\texttt{a})^2(-1+\texttt{e}^2)^2]\\
& -2((1+\texttt{a})(-1+\texttt{e}^2) - 2(-1+\texttt{a})\texttt{z}))
\end{aligned}$$

The graphics representation of the fundamental piece Ω_σ through the immersion ψ^σ is given by the following expression; observe that we leave as variables the parameter $e \in (0,1)$, which measures how much of the end of Ω_σ is represented (the smaller the value of e, the larger size of the represented end) and the parameter σ of the minimal Riemann example.

$$\begin{aligned}
\texttt{r1}[\sigma_][\texttt{e_}] := {} & \texttt{ParametricPlot3D}[\psi[\sigma][\texttt{f}[\texttt{rExp}[\texttt{I Pi t}],\sigma,\texttt{e}]],\{\texttt{r},\texttt{e},1\},\{\texttt{t},0,1\},\\
& \texttt{PlotPoints}->\{40,60\},\texttt{Axes}->\texttt{False}];
\end{aligned}$$

We are now ready to render the fundamental piece that appears in Figure 4, which corresponds to execute the command $\texttt{r1}[2][0.1]$ (i.e., $\sigma = 2$, $e = 0.1$). We type:

$$\texttt{p1} = \texttt{r1}[2][0.1]$$

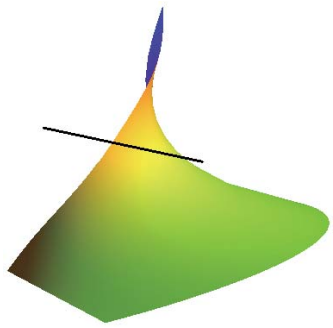

In the last figure, we have also represented a straight line parallel to the x_2-axis, that intersects the surface orthogonally at a point in the boundary of the fundamental piece; the command to render both graphics objects simultaneously is

$$\texttt{p2} = \texttt{Show}[\texttt{p1}, \texttt{line}]$$

where

$$\begin{aligned}\texttt{line} = \texttt{ParametricPlot3D}[&\psi[2][\texttt{Sqrt}[2]\texttt{I}] + \texttt{t}\{0,1,0\}, \{\texttt{t}, -2, 2\},\\ &\texttt{Axes} -> \texttt{False}, \texttt{Boxed} -> \texttt{False},\\ &\texttt{PlotRange} -> \texttt{All}, \texttt{PlotStyle} -> \texttt{Thickness}[0.005]];\end{aligned}$$

produces the line $\psi^\sigma(\sqrt{2}i) + \mathrm{Span}(0,1,0)$. Next we will extend the fundamental piece by 180°-rotation around this line, which induces the holomorphic involution S_1 explained in Section 4.1.1. To define this transformation of the graphic, we will use the command `GeometricTransformation[x, {m, w}]` that applies to a graphics object `x` the affine transformation $x \mapsto mx + w$ (here m is a real 3×3 matrix and $w \in \mathbb{R}^3$ a translation vector). In our case,

$$m = \begin{pmatrix} -1 & 0 & 0 \\ 0 & 1 & 0 \\ 0 & 0 & -1 \end{pmatrix}, \qquad w = (2c_1, 0, 2c_3),$$

where $c = \psi^\sigma(\sqrt{2}i)$. We type:

$$\begin{aligned}\texttt{p3} = \texttt{Graphics3D}[&\texttt{GeometricTransformation}[\texttt{p1}[[1]],\\ &\{\{\{-1,0,0\},\{0,1,0\},\{0,0,-1\}\},\{2\texttt{c1},0,2\texttt{c3}\}\}]];\end{aligned}$$

after having defined `c1` and `c3` as the first and third coordinates of $\psi^\sigma(\sqrt{2}i)$. In order to render the pieces `p1` and `p3` at the same time, as well as the 180°-rotation axis, we type:

$$\texttt{p4} = \texttt{Show}[\texttt{p1}, \texttt{p3}, \texttt{line}]$$

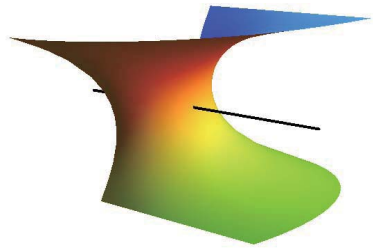

The next step consists of reflecting the last figure in the plane $\{x_2 = 0\}$ (which is the plane orthogonal to the line segments contained in the boundary of the last piece and to the orientation-preserving 180°-rotation axis).

```
p5 = Graphics3D[GeometricTransformation[p4[[1]],
     {{{1, 0, 0}, {0, −1, 0}, {0, 0, 1}}}]];
p6 = Show[p4, p5, line]
```

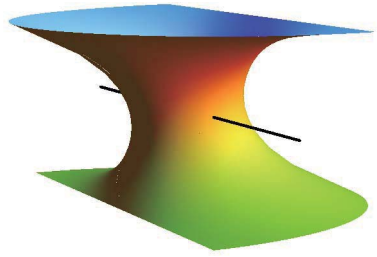

Next we rotate the last piece by angle 180° around the x_2-axis, which is contained in the boundary of the surface.

```
p7 = Graphics3D[GeometricTransformation[p6[[1]],
     {{{−1, 0, 0}, {0, 1, 0}, {0, 0, −1}}}]];
p8 = Show[p6, p7]
```

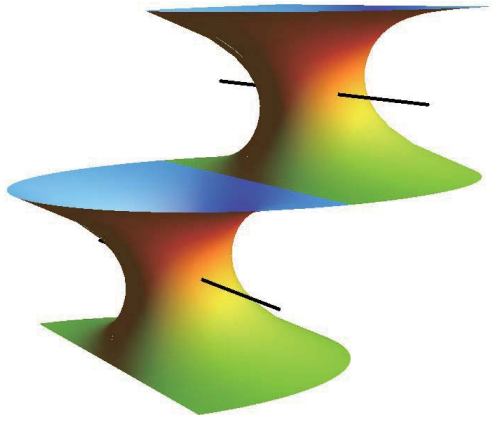

p8 represents a fundamental domain of the Riemann minimal example. The whole surface can be now obtained by translating the graphics domain p8 by multiples of the vector $2\,t_0 = 2\psi^\sigma(-\sigma)$. We define this translation vector t_0:

$$\texttt{t0} = \psi[2][-1.99999]$$

The reason why we have evaluated at a point close to -2 on the right, is due to the aforementioned fact that we must use a continuous branch of the elliptic functions that appear in the expression of ψ. The numeric error that we are making is insignificant with a normal screen resolution. After this translation, we type:

```
p9  = Graphics3D[GeometricTransformation[p8[[1]],
      {{{1,0,0},{0,1,0},{0,0,1}},2 t0}]];
p10 = Show[p8,p9]
```

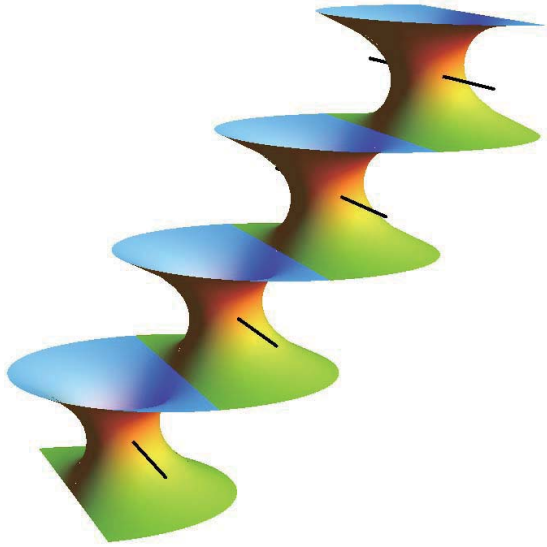

It is desirable to have a better understanding of the surface "at infinity". This can done by taking a smaller value of the parameter e y repeating the whole process. Figure 5 represents the final stage p10 in the case e=0.02. Figure 5 indicates that the surface becomes asymptotic to an infinite family of parallel (actually horizontal) planes, equally spaced. This justifies the wording *planar ends.*

Remark 4.1. For very large or very small values of the parameter σ, one can find imperfections in the graphics, especially around $\psi^\sigma(1)$ or $\psi^\sigma(-\sigma)$. This is due to the fact that these values of σ produce a non-homogeneous distribution of points in the mesh that the program computes when rendering the figure. This issue can be solved by substituting Exp[I Pi t] by Exp[I Pi $\texttt{t}^{\texttt{n}}$] in the definition of r1[σ][z], with n large if σ is close to zero 0, or with n close to zero if σ is large.

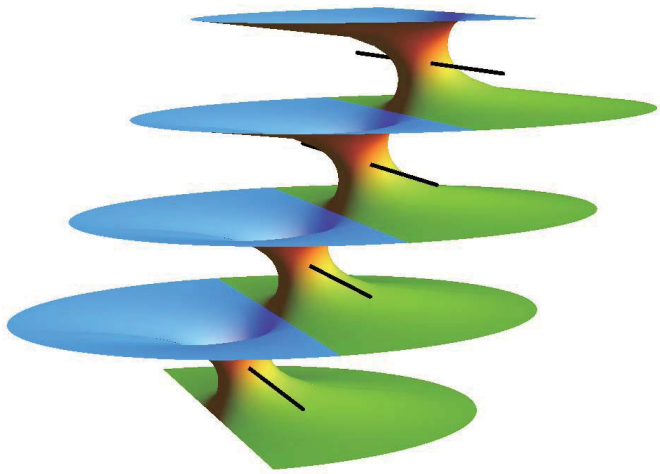

Figure 5: A image of one of the Riemann minimal examples.

5 Uniqueness of the properly embedded minimal planar domains in $\mathbb{R}^3$

As mentioned in Section 4, each Riemann minimal example R_λ is a complete (in fact, proper) embedded minimal surface in $\mathbb{R}^3$ with the topology of a cylinder punctured in an infinite discrete set of points, which is invariant under a translation. If we view this cylinder as a twice punctured sphere, then one deduces that R_λ is topologically (even conformally) equivalent to a sphere minus an infinite set of points that accumulate only at distinct two points, the so called limit ends of R_λ. In particular, R_λ is a planar domain. One longstanding open problem in minimal surface theory has been the following one:

> *Problem: Classify all properly embedded minimal planar domains in* $\mathbb{R}^3$.

Up to scaling and rigid motions, the family $\mathcal{P}$ of all properly embedded planar domains in $\mathbb{R}^3$ comprises the plane, the catenoid, the helicoid and the 1-parameter family of Riemann minimal examples. The proof that this list is complete is a joint effort described in a series of papers by different researchers. In this section we will give an outline of this classification.

5.1 The case of finitely many ends, more than one

One starts by considering a surface $M \in \mathcal{P}$ with k ends, $2 \leq k < \infty$. Even without assuming genus zero, such surfaces of finite genus were proven to have finite total curvature by Collin [6], a case in which the asymptotic geometry is particularly well-understood: the finitely many ends are asymptotic to planes or half-catenoids,

the conformal structure of the surface is the one of a compact Riemann surface minus a finite number of points, and the Gauss map of the surface extends meromorphically to this compactification (Huber [13], Osserman [36]). The asymptotic behavior of the ends and the embeddedness of M forces the values of the extended Gauss map at the ends to be contained in a set of two antipodal points on the sphere. After possibly a rotation in $\mathbb{R}^3$, these values of the extension of the Gauss map of M at the ends can be assumed to be $(0, 0, \pm 1)$. López and Ros [18] found the following argument to conclude that M is either a plane or a catenoid. The genus zero assumption plays a crucial role in the well-posedness of the deformation $\lambda > 0 \mapsto M_\lambda$ of M by minimal surfaces $M_\lambda \subset \mathbb{R}^3$ with the same conformal structure and the same height differential as M but with the meromorphic Gauss map scaled by $\lambda \in [1, \infty)$. A clever application of the maximum principle for minimal surfaces along this deformation implies that all surfaces M_λ are embedded and that if M is not a plane, then M has no points with horizontal tangent planes and no planar ends (because either of these cases produces self-intersections in M_λ for sufficiently large or small values of $\lambda > 0$); in this situation, the third coordinate function of M is proper without critical points, and an application of Morse theory implies that M has the topology of an annulus. From here it is not difficult to prove that M is a catenoid.

5.2 The case of just one end

The next case to consider is when $M \in \mathcal{P}$ has exactly one end, in particular M is topologically a plane, and the goal is to show that M congruent to a plane or to a helicoid. This case was solved by Meeks and Rosenberg [32], by an impressive application of a series of powerful new tools in minimal surface theory: the study of minimal laminations, the so-called Colding-Minicozzi theory and some progresses in the understanding of the conformal structure of complete minimal surfaces. The first two of these tools study the possible limits of a sequence of embedded minimal surfaces under lack of either uniform local area bounds (minimal laminations) or uniform local curvature bounds (Colding-Minicozzi theory) or even both issues happening simultaneously; this is in contrast to the classical situation for describing such limits, that requires both uniform local area and curvature bounds to obtain a classical limit minimal surface.

The study of minimal laminations, carried out in [32] by Meeks and Rosenberg, allows one to relate completeness of embedded minimal surfaces in $\mathbb{R}^3$ to their properness, which is a stronger condition. For instance, in [32] Meeks and Rosenberg proved that if $M \subset \mathbb{R}^3$ is a connected, complete embedded minimal surface with finite topology and bounded Gaussian curvature on compact subdomains of $\mathbb{R}^3$, then M is proper; this properness conclusion was later generalized to the case of finite genus by Meeks, Pérez and Ros in [27], and Colding and Minicozzi [4] proved it in the stronger case that one drops the local boundedness hypothesis for the Gaussian curvature. The theory of minimal laminations has led to other interesting results by itself, see e.g., [15, 16, 20, 21, 24, 25, 29, 33].

Regarding Colding-Minicozzi theory in its relation to the classification by Meeks and Rosenberg of the plane and the helicoid as the only simply connected

elements in $\mathcal{P}$, its main result, called the *Limit Lamination Theorem for Disks,* describes the limit of (a subsequence of) a sequence of compact, embedded minimal disks M_n with boundaries ∂M_n lying in the boundary spheres of Euclidean balls $\mathbb{B}(R_n)$ centered at the origin, where the radii of these balls diverge to ∞, provided that the Gaussian curvatures of the M_n blow up at some sequence of points in $M_n \cap \mathbb{B}(1)$: they proved that this limit is a foliation $\mathcal{F}$ of $\mathbb{R}^3$ by parallel planes, and the convergence of the M_n to $\mathcal{F}$ is of class C^α, $\alpha \in (0,1)$, away from some Lipschitz curve S (called the singular set of convergence of the M_n to $\mathcal{F}$) that intersects each of the planar leaves of $\mathcal{F}$ transversely just once, and arbitrarily close to every point of S, the Gaussian curvature of the M_n also blows up as $n \to \infty$, see [3] for further details. There is another result of fundamental importance in Colding-Minicozzi theory, that is used to prove the Limit Lamination Theorem for Disks and also to demonstrate the results in [4, 27, 32] mentioned in the last paragraph, which is called the *one-sided curvature estimate* [3], a scale invariant bound for the Gaussian curvature of any embedded minimal disk in a half-space.

With all these ingredients in mind, we next give a rough sketch of the proof by Meeks and Rosenberg of the uniqueness of the helicoid as the unique simply connected, properly embedded, nonplanar minimal surface in $\mathbb{R}^3$. Let $M \in \mathcal{P}$ be a simply-connected surface. Consider any sequence of positive numbers $\{\lambda_n\}_n$ which decays to zero and let $\lambda_n M$ be the surface scaled by λ_n. By the Limit Lamination Theorem for Disks, a subsequence of these surfaces converges on compact subsets of $\mathbb{R}^3$ to a minimal foliation $\mathcal{F}$ of $\mathbb{R}^3$ by parallel planes, with singular set of convergence S being a Lipschitz curve that can be parameterized by the height over the planes in $\mathcal{F}$. An application of Colding-Minicozzi theory assures that the limit foliation $\mathcal{F}$ is independent of the sequence $\{\lambda_n\}_n$. After a rotation of M and replacement of the $\lambda_n M$ by a subsequence, one can suppose that the $\lambda_n M$ converge to the foliation $\mathcal{F}$ of $\mathbb{R}^3$ by horizontal planes, outside of the singular set of convergence given by a Lipschitz curve S parameterized by its x_3-coordinate. A more careful analysis of the convergence of $\lambda_n M$ to $\mathcal{F}$ allows also to show that M intersects transversely each of the planes in $\mathcal{F}$. This implies that the Gauss map of M does not take vertical values, so after composing with the stereographical projection we can write this Gauss map $g\colon M \to \mathbb{C} \cup \{\infty\}$ as

$$g(z) = e^{f(z)} \tag{18}$$

for some holomorphic function $f\colon M \to \mathbb{C}$, and the height differential ϕ_3 of M has no zeros or poles. The next step in the proof is to check that the conformal structure of M is $\mathbb{C}$; to see this, first observe that the nonexistence of points in M with vertical normal vector implies that the intrinsic gradient of the third coordinate function $x_3\colon M \to \mathbb{R}$ has no zeros on M. In a delicate argument that uses both the above Colding-Minicozzi picture for limits under shrinkings of M and a finiteness result for the number of components of a minimal graph over a possibly disconnected, proper domain in $\mathbb{R}^2$ with zero boundary values, Meeks and Rosenberg proved that none of the integral curves of ∇x_3 is asymptotic to a plane in $\mathcal{F}$, and that every such horizontal plane intersects M transversely in a single proper arc. This is enough to use the conjugate harmonic function x_3^* of x_3 (which is well-defined on M as the surface is simply connected) to show that

$x_3 + ix_3^*\colon M \to \mathbb{C}$ is a conformal diffeomorphism. Once one knows that M is conformally $\mathbb{C}$, then we can reparameterize conformally M so that

$$\phi_3 = dx_3 + i\, dx_3^* = dz;$$

in particular, the third coordinate $x_3\colon \mathbb{C} \to \mathbb{R}$ is $x_3(z) = \mathrm{Re}(z)$.

To finish the proof, it only remains to determine the Gauss map g of M, of which we now have the description (18) with $f\colon \mathbb{C} \to \mathbb{C}$ entire. If the holomorphic function $f(z)$ is a linear function of the form $az+b$, then one deduces that M is an associate surface[1] to the helicoid; but none of the nontrivial associate surfaces to the helicoid are injective as mappings, which implies that M must be the helicoid itself when $f(z)$ is linear. Thus, the proof reduces to proving that $f(z)$ is linear. The explicit expression for the Gaussian curvature K of M in terms of g, ϕ_3 is

$$K = -\left(\frac{4\,|dg/g|}{(|g| + |g|^{-1})^2 |\phi_3|}\right)^2. \tag{19}$$

Plugging our formulas (18), $\phi_3 = dz$ in our setting, an application of Picard's Theorem to f shows that $f(z)$ is linear if and only if M has bounded curvature. This boundedness curvature assumption for M can be achieved by a clever blow-up argument, thereby finishing the sketch of the proof. For further details, see [32].

5.3 Back to the Riemann minimal examples: the case of infinitely many ends

To finish our outline of the solution of the classification problem stated at the beginning of Section 5, we must explain how to prove that the Riemann minimal examples are the only properly embedded planar domains in $\mathbb{R}^3$ with infinitely many ends.

Let $M \in \mathcal{P}$ be a surface with infinitely many ends. First we analyze the structure of the space $\mathcal{E}(M)$ of ends of M. $\mathcal{E}(M)$ is the quotient $\mathcal{A}/_\sim$ of the set

$$\mathcal{A} = \{\alpha\colon [0,\infty) \to M \mid \alpha \text{ is a proper arc}\}$$

(observe that $\mathcal{A}$ is nonempty as M is not compact) under the following equivalence relation: Given $\alpha_1, \alpha_2 \in \mathcal{A}$, $\alpha_1 \sim \alpha_2$ if for every compact set $C \subset M$, there exists $t_C \in [0,\infty)$ such that $\alpha_1(t), \alpha_2(t)$ lie the same component of $M - C$, for all $t \geq t_C$. Each equivalence class in $\mathcal{E}(M)$ is called a *topological end* of M. If $e \in \mathcal{E}(M)$, $\alpha \in e$ is a representative proper arc and $\Omega \subset M$ is a proper subdomain with compact boundary such that $\alpha \subset \Omega$, then we say that the domain Ω *represents* the end e.

The space $\mathcal{E}(M)$ has a natural topology, which is defined in terms of a basis of open sets: for each proper domain $\Omega \subset M$ with compact boundary, we define the basis open set $B(\Omega) \subset \mathcal{E}(M)$ to be those equivalence classes in $\mathcal{E}(M)$ which have

[1] The family of *associate surfaces* of a simply connected minimal surface with Weierstrass data (g, ϕ_3) are those with the same Gauss map and height differential $e^{i\theta}\phi_3$, $\theta \in [0, 2\pi)$. In particular, the case $\theta = \pi/2$ is the conjugate surface. This notion can be generalized to non-simply connected surfaces, although in that case the associate surfaces may have periods.

representatives contained in Ω. With this topology, $\mathcal{E}(M)$ is a totally disconnected compact Hausdorff space which embeds topologically as a subspace of $[0,1] \subset \mathbb{R}$ (see e.g., pages 288-289 of [22] for a proof of this embedding result for $\mathcal{E}(M)$).

In the particular case that M is a properly embedded minimal surface in $\mathbb{R}^3$ with more than one end, a fundamental result is that $\mathcal{E}(M)$ admits a geometrical ordering by relative heights over a plane called the *limit plane at infinity* of M. To define this reference plane, Callahan, Hoffman and Meeks [1] showed that in one of the closed complements of M in $\mathbb{R}^3$, there exists a noncompact, properly embedded minimal surface Σ with compact boundary and finite total curvature. The ends of Σ are then of catenoidal or planar type, and the embeddedness of Σ forces its ends to have parallel normal vectors at infinity. The limit tangent plane at infinity of M is the plane in $\mathbb{R}^3$ passing through the origin, whose normal vector equals (up to sign) the limiting normal vector at the ends of Σ. It can be proved that such a plane does not depend on the finite total curvature minimal surface $\Sigma \subset \mathbb{R}^3 - M$ [1]. With this notion in hand, the ordering theorem is stated as follows.

Theorem 5.1. (Ordering Theorem, Frohman, Meeks [10]) *Let $M \subset \mathbb{R}^3$ be a properly embedded minimal surface with more than one end and horizontal limit tangent plane at infinity. Then, the space $\mathcal{E}(M)$ of ends of M is linearly ordered geometrically by the relative heights of the ends over the (x_1, x_2)-plane, and embeds topologically in $[0,1]$ in an ordering preserving way. Furthermore, this ordering has a topological nature in the following sense: If M is properly isotopic to a properly embedded minimal surface M' with horizontal limit tangent plane at infinity, then the associated ordering of the ends of M' either agrees with or is opposite to the ordering coming from M.*

Given a minimal surface $M \subset \mathbb{R}^3$ satisfying the hypotheses of Theorem 5.1, we define the *top end* e_T of M as the unique maximal element in $\mathcal{E}(M)$ for the ordering given in this theorem (as $\mathcal{E}(M) \subset [0,1]$ is compact, then e_T exists). Analogously, the *bottom end* e_B of M is the unique minimal element in $\mathcal{E}(M)$. If $e \in \mathcal{E}(M)$ is neither the top nor the bottom end of M, then it is called a *middle end* of M. There is another way of grouping ends of such a surface M into simple and limit ends; for the sake of simplicity and as we are interested in discussing the classification of surfaces $M \in \mathcal{P}$, we will restrict in the sequel to the case of a surface M of genus zero.

Given $M \in \mathcal{P}$, an isolated point $e \in \mathcal{E}(M)$ is called a *simple end of* M, and e can be represented by a proper subdomain $\Omega \subset M$ with compact boundary which is homeomorphic to the annulus $\mathbb{S}^1 \times [0, \infty)$. Because of this model, e is also called an *annular end.* On the contrary, ends in $\mathcal{E}(M)$ which are not simple (i.e., they are limit points of $\mathcal{E}(M) \subset [0,1]$) are called *limit ends* of M. In our situation of M being a planar domain, its limit ends can be represented by proper subdomains $\Omega \subset M$ with compact boundary, genus zero and infinitely many ends. As in this section M is assumed to have infinitely many ends and $\mathcal{E}(M)$ is compact, then M must have at least one limit end.

Each of the planar ends of a Riemann minimal example R_λ is a simple annular middle end, and R_λ has two limit ends corresponding to the limits of planar ends

as the height function of R_λ goes to ∞ (this is the top end of R_λ) or to $-\infty$ (bottom end). Thus, middle ends of R_λ correspond to simple ends, and its top and bottom ends are limit ends. Most of this behavior is in fact valid for any properly embedded minimal surface $M \subset \mathbb{R}^3$ with more than one end:

Theorem 5.2 (Collin, Kusner, Meeks, Rosenberg [7]). *Let $M \subset \mathbb{R}^3$ be a properly embedded minimal surface with more than one end and horizontal limit tangent plane at infinity. Then, any limit end of M must be a top or bottom end of M. In particular, M can have at most two limit ends, each middle end is simple and the number of ends of M is countable.*

In the sequel, we will assume that our surface $M \in \mathcal{P}$ has horizontal limit tangent plane at infinity. By Theorem 5.2, M has no middle limit ends, hence either it has one limit end (this one being its top or its bottom limit end) or both top and bottom ends are the limit ends of M, like in a Riemann minimal example. The next step in our description of the classification of surfaces in $\mathcal{P}$ is due to Meeks, Pérez and Ros [28], who discarded the one limit end case through the following result.

Theorem 5.3 (Meeks, Pérez, Ros [28]). *If $M \subset \mathbb{R}^3$ is a properly embedded minimal surface with finite genus, then M cannot have exactly one limit end.*

The proof of Theorem 5.3 is by contradiction. One assumes that the set of ends of M, linearly ordered by increasing heights by the Ordering Theorem 5.1, is $\mathcal{E}(M) = \{e_1, e_2, \ldots, e_\infty\}$ with the limit end of M being its top end e_∞. Each annular end of M is a simple end and can be proven to be asymptotic to a graphical annular end E_n of a vertical catenoid with negative logarithmic growth a_n satisfying $a_1 \leq \ldots \leq a_n \leq \ldots < 0$ (Theorem 2 in Meeks, Pérez and Ros [27]). Then one studies the subsequential limits of homothetic shrinkings $\{\lambda_n M\}_n$, where $\{\lambda_n\}_n \subset \mathbb{R}^+$ is any sequence of numbers decaying to zero; recall that this was also a crucial step in the proof of the uniqueness of the helicoid sketched in Section 5.2. Nevertheless, the situation now is more delicate as the surfaces $\lambda_n M$ are not simply connected. Instead, it can be proved that the sequence $\{\lambda_n M\}_n$ is *locally simply connected* in $\mathbb{R}^3 - \{\vec{0}\}$, in the sense that given any point $p \in \mathbb{R}^3 - \{\vec{0}\}$, there exists a number $r(p) \in (0, |p|)$ such that the open ball $\mathbb{B}(p, r(p))$ centered at p with radius $r(p)$ intersects $\lambda_n M$ in compact disks whose boundaries lie on $\partial\mathbb{B}(p, r(p))$, for all $n \in \mathbb{N}$. This is a difficult technical part of the proof, where the Colding-Minicozzi theory again plays a crucial role. Then one uses this locally simply connected property in $\mathbb{R}^3 - \{0\}$ to show that the limits of subsequences of $\{\lambda_n M\}_n$ consist of minimal laminations $\mathcal{L}$ of $H(*) = \{x_3 \geq 0\} - \{\vec{0}\} \subset \mathbb{R}^3$ containing $\partial H(*)$ as a leaf, and that the singular set of convergence of the of $\lambda_n M$ to $\mathcal{L}$ is empty; from here one has that

> ($\star$) The sequence $\{|K_{\lambda_n M}|\}_n$ of absolute Gaussian curvature functions of the $\lambda_n M$, is locally bounded in $\mathbb{R}^3 - \{0\}$.

In particular, taking $\lambda_n = |p_n|^{-1}$ where p_n is any divergent sequence of points on M, ($\star$) implies that the absolute Gaussian curvature of M decays at least

quadratically in terms of the distance function $|p_n|$ to the origin. In this setting, the Quadratic Curvature Decay Theorem stated in Theorem 5.4 below implies that M has finite total curvature; this is impossible in our situation with infinitely many ends, which finishes our sketch of proof of Theorem 5.3.

Theorem 5.4. (Quadratic Curvature Decay Theorem, Meeks, Pérez, Ros [24]) *Let $M \subset \mathbb{R}^3 - \{\vec{0}\}$ be an embedded minimal surface with compact boundary (possibly empty), which is complete outside the origin $\vec{0}$; i.e., all divergent paths of finite length on M limit to $\vec{0}$. Then, M has quadratic decay of curvature*[2] *if and only if its closure in $\mathbb{R}^3$ has finite total curvature.*

Once we have discarded the case of a surface $M \in \mathcal{P}$ with just one limit end, it remains to prove that when M has two limit ends, then M is a Riemann minimal example. The argument for proving this is also delicate, but since it uses strongly the Shiffman function and its surprising connection to the theory of integrable systems and more precisely, to the Korteweg-de Vries equation, we will include some details of it.

We first need to establish a framework for M which makes possible to use globally the Shiffman function; here the word *globally* also refers its *extension across the planar ends* of M, in a strong sense to be precise soon. Recall that we have normalized M so that its limit tangent plane at infinity is the (x_1, x_2)-plane. By Theorem 5.2, the middle ends of M are not limit ends, and as M has genus zero, then these middle ends can be represented by annuli. Since M has more than one end, then every annular end of M has finite total curvature (by Collin's theorem [6], that we also used at the beginning of Section 5.1), and thus such annular ends of M are asymptotic to the ends of planes or catenoids. Now recall Theorem 5.2 above, due to Collin, Kusner, Meeks and Rosenberg. The same authors obtained in [7] the following additional information about the middle ends:

Theorem 5.5 (Theorem 3.5 in [7])**.** *Suppose a properly embedded minimal surface Σ in $\mathbb{R}^3$ has two limit ends with horizontal limit tangent plane at infinity. Then there exists a sequence of horizontal planes $\{P_j\}_{j\in\mathbb{N}}$ in $\mathbb{R}^3$ with increasing heights, such that Σ intersects each P_j transversely in a compact set, every middle end of Σ has an end representative which is the closure of the intersection of Σ with the slab bounded by $P_j \cup P_{j+1}$, and every such slab contains exactly one of these middle end representatives.*

Theorem 5.5 gives a way of separating the middle ends of M into regions determined by horizontal slabs, in a similar manner as the planar ends of a Riemann minimal example can be separated by slabs bounded by horizontal planes. Furthermore, the Half-space Theorem [12] by Hoffman and Meeks ensures that the restriction of the third coordinate function x_3 to the portion $M(+)$ of M above P_0 is not bounded from above and extends smoothly across the middle ends. Another crucial result, Theorem 3.1 in [7], implies that $M(+)$ is conformally parabolic (in the sense that Brownian motion on $M(+)$ is recurrent), in particular the annular simple middle ends of M in $M(+)$ are conformally punctured disks. After

[2]This means that $|K_M|R^2$ is bounded on M, where $R^2 = x_1^2 + x_2^2 + x_3^2$.

compactification of $M(+)$ by adding its middle ends and their limit point p_∞ corresponding to the top end of M, we obtain a conformal parameterization of this compactification defined on the unit disk $\mathbb{D} = \{|z| \leq 1\}$, so that $p_\infty = 0$, the middle ends in $M(+)$ correspond to a sequence of points $p_j \in \mathbb{D} - \{0\}$ converging to zero as $j \to \infty$, and

$$x_3|_{M(+)}(z) = -\lambda \ln |z| + c$$

for some $\lambda, c \in \mathbb{R}$, $\lambda > 0$. This implies that there are no points in $M(+)$ with horizontal tangent plane. Observe that different planar ends in M cannot have the same height above P_0 by Theorem 5.5, which implies that $M(+)$ intersects every plane P' above P_0 in a simple closed curve if the height of P' does not correspond to the height of any middle end, while P' intersects $M(+)$ is a proper Jordan arc when the height of P' equals the height of a middle end. Similar reasoning can be made for the surface $M(-) = M - [M(+) \cup P_0]$. From here one deduces easily that the meromorphic extension through the planar ends of the stereographically projected Gauss map g of M has order-two zeros and poles at the planar ends, and no other zeros or poles in M. This is a sketch of the proof of the first four items of the following descriptive result, which is part of Theorem 1 in [27].

Theorem 5.6. *Let $M \in \mathcal{P}$ be a surface with infinitely many ends. Then, after a rotation and a homothety we have:*

1. *M can be conformally parameterized by the cylinder $\mathbb{C}/\langle i \rangle$ punctured in an infinite discrete set of points $\{p_j, q_j\}_{j \in \mathbb{Z}}$ which correspond to the planar ends of M.*

2. *The stereographically projected Gauss map $g\colon (\mathbb{C}/\langle i \rangle) - \{p_j, q_j\}_{j \in \mathbb{Z}} \to \mathbb{C} \cup \{\infty\}$ extends through the planar ends of M to a meromorphic function g on $\mathbb{C}/\langle i \rangle$ which has double zeros at the points p_j and double poles at the q_j.*

3. *The height differential of M is $\phi_3 = dz$ with z being the usual conformal coordinate on $\mathbb{C}$, hence the third coordinate function of M is $x_3(z) = \mathrm{Re}(z)$.*

4. *The planar ends of M are ordered by their heights so that $\mathrm{Re}(p_j) < \mathrm{Re}(q_j) < \mathrm{Re}(p_{j+1})$ for all j with $\mathrm{Re}(p_j) \to \infty$ (resp. $\mathrm{Re}(p_j) \to -\infty$) when $j \to \infty$ (resp. $j \to -\infty$).*

The description in Theorem 5.6 allows us to define globally the Shiffman function on any surface M as in that theorem. To continue our study of properties of such a surface, we need the notion of *flux*. The flux vector along a closed curve $\gamma \subset M$ is defined as

$$F(\gamma) = \int_\gamma \mathrm{Rot}_{90^\circ}(\gamma') = \mathrm{Im} \int_\gamma \left(\frac{1}{2}\left(\frac{1}{g} - g\right), \frac{i}{2}\left(\frac{1}{g} + g\right), 1 \right) \phi_3, \qquad (20)$$

where (g, ϕ_3) is the Weierstrass data of M and Rot_{90° denotes the rotation by angle $\pi/2$ in the tangent plane of M at any point. It is easy to show that $F(\gamma)$ only depends of the homology class of γ in M, and that the flux along a closed curve that encloses a planar end of M is zero. In particular, for a surface M as

in Theorem 5.6, the only flux vector to consider is that associated to any compact horizontal section $M \cap \{x_3 = \text{constant}\}$, which we will denote by $F(M)$. Note that by item (3) of Theorem 5.6, the third component of $F(M)$ is 1. In the sequel, we will assume the following normalization for M after possibly a rotation in $\mathbb{R}^3$ around the x_3-axis:

$$F(M) = (h, 0, 1) \text{ for some } h \geq 0. \tag{21}$$

The next result collects some more subtle properties of a surface M as in Theorem 5.6 (this is the second part of Theorem 1 in [27]).

Theorem 5.7. *For a surface M normalized as in (21), we have:*

5. *The flux vector $F(M)$ of M along a compact horizontal section has nonzero horizontal component; equivalently, $F(M) = (h, 0, 1)$ for some $h > 0$.*

6. *The Gaussian curvature of M is bounded and the vertical spacings between consecutive planar ends are bounded from above and below by positive constants, with all these constants depending only on h.*

7. *For every divergent sequence $\{z_k\}_k \subset \mathbb{C}/\langle i\rangle$, there exists a subsequence of the meromorphic functions $g_k(z) = g(z + z_k)$ which converges uniformly on compact subsets of $\mathbb{C}/\langle i\rangle$ to a non-constant meromorphic function $g_\infty \colon \mathbb{C}/\langle i\rangle \to \mathbb{C} \cup \{\infty\}$ (we will refer to this property saying that g is quasi-periodic). In fact, g_∞ corresponds to the Gauss map of a minimal surface M_∞ satisfying the same properties and normalization (21) as M, which is the limit of a related subsequence of translations of M by vectors whose x_3-components are $\mathrm{Re}(z_k)$.*

As said above, the proof of properties 5, 6 and 7 are more delicate than the ones in Theorem 5.6 as they depend on Colding-Minicozzi theory. For instance, the fact that the Gaussian curvature K_M of M is bounded with the bound depending only on an upper bound of the horizontal component of $F(M)$, was proven in Theorem 5 of [27] in the more general case of a sequence $\{M_k\}_k \subset \mathcal{P}$ as in Theorem 5.6, such that $F(M_k) = (h_k, 0, 1)$ and $\{h_k\}_k$ is bounded from above. This proof of the existence of a uniform curvature estimate is by contradiction: the existence of a sequence $p_k \in M_k$ such that $|K_{M_k}|(p_k) \to \infty$ creates a nonflat blow-up limit of the M_k around p_k with can be proven to be a vertical helicoid (this uses the uniqueness of the helicoid among properly embedded, simply connected, nonflat minimal surfaces, see Section 5.2). A careful application of the so called *Limit Lamination Theorem for Planar Domains* (Theorem 0.9 in Colding and Minicozzi [5]) produces a sequence $\mu_k > 0$ so that after possibly a sequence of translations and rotations around a vertical axis, $\{\mu_k M_k\}_k$ converges to a foliation of $\mathbb{R}^3$ by horizontal planes with singular set of convergence consisting of two vertical lines $\Gamma \cup \Gamma'$ separated by a positive distance. From here one can produce a nontrivial closed curve in each $\mu_k M_k$ such that the flux vector $F(\mu_k M_k)$ converges as $k \to \infty$ to twice the horizontal vector that joins Γ and Γ'. Since the angle between $F(M_k)$ and its horizontal projection $(h_k, 0, 0)$ is invariant under translations, homotheties and rotations around the x_3-axis, then we contradict that h_k is bounded from above.

The proof that there is a lower bound of the vertical spacings between consecutive planar ends in item 6 of Theorem 5.7 follows from that fact that the boundedness of K_M implies the existence of an embedded regular neighborhood of constant radius (Meeks and Rosenberg [31]). The bound from above of the same vertical spacing is again proved by contradiction, by a clever application of the López-Ros deformation argument (see Section 5.1), which also gives property 5 of Theorem 5.7. Finally, the proof of the compactness result in item 7 of Theorem 5.7 is essentially a consequence of the already proven uniform bound of the Gaussian curvatures and the uniform local bounds for the area of a sequence of translations of the surface M given by item 6 of the same theorem. This completes our sketch of proof of Theorem 5.7.

As explained above, in our setting for $M \in \mathcal{P}$ satisfying the normalizations in Theorems 5.6 and 5.7, we can consider its Shiffman function S_M defined by equation (17), which is also defined on the conformal compactification of M (recall that in Section 4.2 we normalized the height differential ϕ_3 to be dz, as in Theorem 5.6). Recall also that the vanishing of the Shiffman function is equivalent to the fact that M is a Riemann minimal example. But instead of proving directly that $S_M = 0$ on M, Meeks, Pérez and Ros demonstrated that S_M is a linear Jacobi function; to understand this concept, we must first recall some basic facts about Jacobi functions on a minimal surface.

Since minimal surfaces can be viewed as critical points for the area functional A, the nullity of the hessian of A at a minimal surface M contains valuable information about the geometry of M. Normal variational fields for M can be identified with functions, and the second variation of area tells us that the functions in the nullity of the hessian of A coincide with the kernel of the *Jacobi operator*, which is the Schrödinger operator on M given by

$$L = \Delta - 2K_M, \tag{22}$$

where Δ denotes the intrinsic Laplacian on M. Any function $v \in C^\infty(M)$ satisfying $\Delta v - 2K_M v = 0$ on M is called a *Jacobi function,* and corresponds to an *infinitesimal* deformation of M by minimal surfaces. It turns out that the Shiffman function S_M is a Jacobi function, i.e., it satisfies (22) (this is general for any minimal surface whenever S_M is well-defined, and follows by direct computation from (17)). One obvious way to produce Jacobi fields is to take the normal part of the variational field of the variation of M by moving it through a 1-parameter family of isometries of $\mathbb{R}^3$. For instance, the translations $M + ta$ with $a \in \mathbb{R}^3$, produce the Jacobi function $\langle N, a\rangle$ (here N is the Gauss map of M), which is called *linear Jacobi function.* One key step in the proof of Meeks, Pérez and Ros is the following one.

Proposition 5.8. *Let $M \in \mathcal{P}$ be a surface with infinitely many ends and satisfying the normalizations in Theorems 5.6 and 5.7. If the Shiffman Jacobi function S_M of M is linear, i.e., $S_M = \langle N, a\rangle$ for some $a \in \mathbb{R}^3$, then M is a Riemann minimal example.*

The proof of Proposition 5.8 goes as follows. We first pass from real valued Jacobi functions to complex valued ones by means of the *conjugate of a Jacobi*

function. The conjugate function of a Jacobi function u over a minimal surface M is the (locally defined) support function $u^* = \langle (X_u)^*, N\rangle$ of the conjugate surface[3] $(X_u)^*$ of the branched minimal surface X_u associated to u by the so-called Montiel-Ros correspondence [34]; in particular, both X_u and $(X_u)^*$ have the same Gauss map N as M, and u^* also satisfies the Jacobi equation. Now suppose $M \in \mathcal{P}$ is an Proposition 5.8, i.e., S_M is linear. It is then easy to show that the conjugate Jacobi function $(S_M)^*$ of S_M, is also linear, from where $S_M + iS_M^* = \langle N, a\rangle$ for some $a \in \mathbb{C}^3$, which again by (17), produces a complex ODE for g of second order, namely

$$\overline{g}\left(\frac{3}{2}\frac{(g')^2}{g} - g'' - B - a_3 g\right) = \frac{g''}{g} - \frac{1}{2}\left(\frac{g'}{g}\right)^2 + Ag - a_3, \tag{23}$$

for some complex constants A, B, a_3 that only depend of a. As g is holomorphic and not constant, (23) implies that both its right-hand side and the expression between parenthesis in its left-hand side vanish identically. Solving for g'' in both equations, one arrives to the following complex ODE of first order:

$$(g')^2 = g(-Ag^2 + 2a_3 g + B),$$

which in turn says that the Weierstrass data $(g, \phi_3 = dz)$ of M factorizes through the torus $\Sigma = \{(\xi, w) \in (\mathbb{C}\cup\{\infty\})^2 \mid w^2 = \xi(-A\xi^2 + 2a_3\xi + B)\}$; in other words, we deduce that M is in fact periodic under a translation, with a quotient being a twice punctured torus. In this very particular situation, one can apply the classification of periodic examples by Meeks, Pérez and Ros in [26] to conclude that M is a Riemann minimal example, and the proposition is proved.

In light of Proposition 5.8, one way of finishing our classification problem consists of proving the following statement, which will be proved assuming that Theorem 5.10 stated immediately after it holds; the proof of Theorem 5.10 will be sketched later.

Proposition 5.9. *For every $M \in \mathcal{P}$ with infinitely many ends and satisfying the normalizations in Theorems 5.6, 5.7 and in (21), the Shiffman Jacobi function S_M of M is linear.*

Theorem 5.10 (Theorem 5.14 in [30])**.** *Given a surface $M \in \mathcal{P}$ with infinitely many ends and satisfying the normalizations in Theorems 5.6 and 5.7, there exists a 1-parameter family $\{M_t\}_t \subset \mathcal{P}$ such that $M_0 = M$ and the normal part of the variational field for this variation, when restricted to each M_t, is the Shiffman function S_{M_t} multiplied by the unit normal vector field to M_t.*

Before proving Proposition 5.9, some explanation about the integration of the Shiffman function S_M appearing in Theorem 5.10 is in order. As we explained in the paragraph just before the statement of Proposition 5.8, S_M corresponds to an *infinitesimal* deformation of M by minimal surfaces (every Jacobi function has this property). But this is very different from the quite strong property of

[3]The conjugate surface of a minimal surface is that one whose coordinate functions are harmonic conjugates of the coordinate functions of the original minimal surface; the conjugate surface is only locally defined, and it is always minimal.

proving that S_M can be integrated to an actual variation $t \mapsto M_t \in \mathcal{P}$, as stated in Theorem 5.10. Even more, the parameter t of this deformation can be proven to extend to be a complex number in $\mathbb{D}(\varepsilon) = \{t \in \mathbb{C} \mid |t| < \varepsilon\}$ for some $\varepsilon > 0$, and $t \in \mathbb{D}(\varepsilon) \mapsto M_t$ can be viewed as the real part of a complex valued *holomorphic* curve in a certain complex variety. This is a very special integration property for S_M, which we refer to by saying that the Shiffman function can be *holomorphically integrated* for every surface M as in Theorem 5.10.

We next give a sketch of the proof of Proposition 5.9, assuming the validity of Theorem 5.10. One fixes a flux vector $F = (h, 0, 1)$, $h > 0$, consider the set

$$\mathcal{P}_F = \{M \in \mathcal{P} \text{ as in Theorems 5.6 and 5.7 } \mid F(M) = F\}$$

and maximize the spacing between the planar ends of surfaces in $\mathcal{P}_F$ (to do this one needs to be careful when specifying what planar ends are compared when measuring distances; we will not enter in technical details here), which can be done by the compactness property given in item 6 of Theorem 5.7. Then one proves that any maximizer (not necessarily unique a priori) $M_{\max} \in \mathcal{P}_F$ must have linear Shiffman function; the argument for this claim has two steps:

(S1) The assumed homomorphic integration of the Shiffman function of $M_{\max}$ produces a complex holomorphic curve $t \in \mathbb{D}(\varepsilon) \mapsto g_t \in \mathcal{W}$, with $g_0 = g_{\max}$ being the Gauss map of $M_{\max}$, where $\mathcal{W}$ is the complex manifold of quasi-periodic meromorphic functions on $\mathbb{C}/\langle i \rangle$ (in the sense explained in item 7 of Theorem 5.7) with double zeros and double poles; $\mathcal{W}$ can be identified to the set of potential Weierstrass data of minimal immersions $(g, \phi_3 = dz)$ with infinitely many planar ends. The fact that the period problem associated to (g_t, dz) is solved for any t comes from the fact that for $t = 0$, this period problem is solved (as $M_{\max}$ is a genuine surface) and that the velocity vector of $t \mapsto g_t$ is the Shiffman function at any value of t, which lies in the kernel of the period map. A similar argument shows that not only (g_t, dz) solve the period problem, but also the flux vector $F(M_t)$ is independent of t, where M_t is the minimal surface produced by the Weierstrass data (g_t, dz) (thus $M_0 = M_{\max}$). Embeddedness of M_t is guaranteed from that of $M_{\max}$, by the application of the maximum principle for minimal surfaces. Altogether, we deduce that $t \in \mathbb{D}(\varepsilon) \mapsto M_t$ actually lies in $\mathcal{P}_F$, which implies that the spacing between the planar ends of M_t, viewed as a function of t, achieves a maximum at $t = 0$.

(S2) As the spacing between the planar ends of M_t can be viewed as a harmonic function of t (this follows from item 4 of Theorem 5.6), then the maximizing property of $M_{\max}$ in the family $t \in \mathbb{D}(\varepsilon) \mapsto M_t$ and the maximum principle for harmonic functions gives that the spacing between the planar ends of M_t remains constant in t; from here it is not difficult to deduce that $t \mapsto g_t$ is just a translation in the cylinder $\mathbb{C}/\langle i \rangle$ of the zeros and poles of g_t, which corresponds geometrically to the fact that $t \mapsto M_t$ is a translation in $\mathbb{R}^3$ of $M_{\max}$. Therefore, the velocity vector of $t \mapsto M_t$ at $t = 0$, which is the Shiffman function of $M_{\max}$, is linear.

Once it is proven that the Shiffman function of $M_{\max}$ is linear, Proposition 5.8 implies that $M_{\max}$ is a Riemann minimal example. A similar reasoning can be done for a minimizer $M_{\min} \in \mathcal{P}_F$ of the spacing between planar ends, hence $M_{\min}$ is also a Riemann minimal example. As there is only one Riemann example for each flux F, then we deduce that the maximizer and minimizer are the same. In particular, every surface in $\mathcal{P}_F$ is both a maximizer and minimizer and, hence, its Shiffman function is linear. This finishes the sketch of proof of Proposition 5.9.

To finish this article, we will indicate how to demonstrate that the Shiffman function of every surface $M \in \mathcal{P}$ in the hypotheses of Theorem 5.10 can be holomorphically integrated. This step is where the Korteweg-de Vries equation (KdV) plays a crucial role, which we will explain now. We recommend the interested reader to consult the excellent survey by Gesztesy and Weikard [11] for an overview of the notions and properties that we will use in the sequel.

First we explain the connection between the Shiffman function and the KdV equation. Let $M \in \mathcal{P}$ be a surface satisfying the hypotheses of Theorem 5.10, and let S_M be its Shiffman function, which is globally defined. Its conjugate Jacobi function $(S_M)^*$ is also globally defined; in fact, $(S_M)^*$ is given by minus the real part of the expression enclosed between brackets in (17). By the Montiel-Ros correspondence [34], both S_M, $(S_M)^*$ can be viewed as the support functions of conjugate branched minimal immersions $X, X^* \colon M \to \mathbb{R}^3$ with the same Gauss map as M. The holomorphicity of $X + iX^*$ allows us to identify $S_M + iS_M^*$ with an infinitesimal deformation of the Gauss map g of M in the space $\mathcal{W}$ of quasi-periodic meromorphic functions on $\mathbb{C}/\langle i\rangle$ that appears in step (S1) above. In other words, $S_M + iS_M^*$ can be viewed as the derivative $\dot{g}_S = \frac{d}{dt}\big|_{t=0} g_t$ of a holomorphic curve $t \in \mathbb{D}(\varepsilon) = \{t \in \mathbb{C} \mid |t| < \varepsilon\} \mapsto g_t \in \mathcal{W}$ with $g_0 = g$, which can be explicitly computed from (17) as

$$\dot{g}_S = \frac{i}{2}\left(g''' - 3\frac{g'g''}{g} + \frac{3}{2}\frac{(g')^3}{g^2}\right). \tag{24}$$

Therefore, to integrate S_M holomorphically one needs to find a holomorphic curve $t \in \mathbb{D}(\varepsilon) \mapsto g_t \in \mathcal{W}$ with $g_0 = g$, such that for all t, the pair $(g_t, \phi_3 = dz)$ is the Weierstrass data of a minimal surface $M_t \in \mathcal{P}$ satisfying the conditions of Theorem 5.10, and such that for every value of t,

$$\left.\frac{d}{dt}\right|_t g_t = \frac{i}{2}\left(g_t''' - 3\frac{g_t' g_t''}{g_t} + \frac{3}{2}\frac{(g_t')^3}{g_t^2}\right).$$

Viewing (24) as an evolution equation in complex time t, one could apply general techniques to find solutions $g_t = g_t(z)$ defined locally around a point $z_0 \in (\mathbb{C}/\langle i\rangle) - g^{-1}(\{0,\infty\})$ with the initial condition $g_0 = g$, but such solutions are not necessarily defined on the whole cylinder, can develop essential singularities, and even if they were meromorphic on $\mathbb{C}/\langle i\rangle$, it is not clear *a priori* that they would have only double zeros and poles and other properties necessary to give rise, via the Weierstrass representation with height differential $\phi_3 = dz$, to minimal surfaces M_t in $\mathcal{P}$ with infinitely many planar ends. Fortunately, all of these problems can be solved by arguments related to the theory of the meromorphic KdV equation.

The change of variables

$$u = -\frac{3(g')^2}{4g^2} + \frac{g''}{2g}. \tag{25}$$

transforms (24) into the evolution equation

$$\frac{\partial u}{\partial t} = -u''' - 6uu', \tag{26}$$

which is the celebrated KdV equation[4]. The apparently magical change of variables (25) has a natural explanation: the change of variables $x = g'/g$ transforms the expression (24) for $\dot{g}_S$ into the evolution equation

$$\dot{x} = \frac{i}{2}(x''' - \frac{3}{2}x^2x'),$$

which is called a *modified KdV equation* (mKdV). It is well-known that mKdV equations in x can be transformed into KdV equations in u through the so called *Miura transformations,* $x \mapsto u = ax' + bx^2$ with a, b suitable constants, see for example [11] page 273. Equation (25) is nothing but the composition of $g \mapsto x$ and a Miura transformation. The holomorphic integration of the Shiffman function S_M could be performed just in terms of the theory of the mKdV equation, but we will instead use the more standard KdV theory.

Coming back to the holomorphic integration of S_M, this problem amounts to solving globally in $\mathbb{C}/\langle i\rangle$ the Cauchy problem for equation (26), i.e.,

> Problem. Find a meromorphic solution $u(z,t)$ of (26) defined for $z \in \mathbb{C}/\langle i\rangle$ and $t \in \mathbb{D}(\varepsilon)$, whose initial condition is $u(z,0) = u(z)$ given by (25).

It is a well-known fact in KdV theory (see for instance [11] and also see Segal and Wilson [38]) that the above Cauchy problem can be solved globally producing a holomorphic curve $t \mapsto u_t$ of meromorphic functions $u(z,t) = u_t(z)$ on $\mathbb{C}/\langle i\rangle$ with controlled Laurent expansions in poles of u_t, provided that the initial condition $u(z)$ is an *algebro-geometric potential* for the KdV equation (to be defined below); a different question is whether or not this family $u_t(z)$ solves our geometric problem related to minimal surfaces in $\mathcal{P}$.

To understand the notion of algebro-geometric potential, one must view (26) as the level $n = 1$ in a sequence of evolution equations in u, called the *KdV hierarchy,*

$$\left\{ \frac{\partial u}{\partial t_n} = -\partial_z \mathcal{P}_{n+1}(u) \right\}_{n\geq 0}, \tag{27}$$

where $\mathcal{P}_{n+1}(u)$ is a differential operator given by a polynomial expression of u and its derivatives with respect to z up to order $2n$. These operators, which are closely related to Lax Pairs (see Section 2.3 in [11]) are defined by the recurrence law

$$\begin{cases} \partial_z \mathcal{P}_{n+1}(u) = (\partial_{zzz} + 4u\,\partial_z + 2u')\mathcal{P}_n(u), \\ \mathcal{P}_0(u) = \frac{1}{2}. \end{cases} \tag{28}$$

[4]One can find different normalizations of the KdV equation in the literature, given by different coefficients for u''', uu' in equation (26); all of them are equivalent up to a change of variables.

In particular, $\mathcal{P}_1(u) = u$ and $\mathcal{P}_2(u) = u'' + 3u^2$ (plugging $\mathcal{P}_2(u)$ in (27) one obtains the KdV equation). Hence, for each $n \in \mathbb{N} \cup \{0\}$, one must consider the right-hand side of the n-th equation in (27) as a polynomial expression of $u = u(z)$ and its derivatives with respect to z up to order $2n + 1$. We will call this expression a *flow*, denoted by $\frac{\partial u}{\partial t_n}$. A function $u(z)$ is said to be an *algebro-geometric potential* of the KdV equation if there exists a flow $\frac{\partial u}{\partial t_n}$ which is a linear combination of the lower order flows in the KdV hierarchy.

Once we understand the notion of algebro-geometric potential for the KdV equation, we have divided our goal of proving the holomorphic integration of the Shiffman function for any surface M as in Theorem 5.10 into two final steps.

(T1) For every minimal surface $M \in \mathcal{P}$ satisfying the hypotheses of Theorem 5.10, the function $u = u(z)$ defined by equation (25) in terms of the Gauss map $g(z)$ of M, is an algebro-geometric potential of the KdV equation. This step would then give a meromorphic solution $u(z,t) = u_t(z)$ of the KdV flow (26) defined for $z \in \mathbb{C}/\langle i \rangle$ and $t \in \mathbb{D}(\varepsilon)$, with initial condition $u(z,0) = u(z)$ given by (25).

(T2) With $u_t(z)$ as in (T1), it is possible to define a holomorphic curve $t \mapsto g_t \in \mathcal{W}$ with $g_0 = g$ (recall that g is the stereographic projection of the Gauss map of M), such that $(g_t, \phi_3 = dz)$ solves the period problem and defines a minimal surface $M_t \in \mathcal{P}$ that satisfies the conclusions of Theorem 5.10.

Property (T1) follows from a combination of the following two facts:

(a) Each flow $\frac{\partial u}{\partial t_n}$ in the KdV hierarchy (27) produces a *bounded,* complex valued Jacobi function v_n on $\mathbb{C}/\langle i \rangle$ in a similar manner to the way that the flow $\frac{\partial u}{\partial t_1}$ produces the complex Shiffman function $S_M + iS_M^*$.

(b) Since the Jacobi functions v_n produced in item (a) are bounded on $\mathbb{C}/\langle i \rangle$ and the Jacobi operator (22) is the Shrödinger operator given by (22) on M, then the v_n can be considered to lie in the kernel of a Schrödinger operator L_M on $\mathbb{C}/\langle i \rangle$ with bounded potential; namely, $L_M = (\Delta_{\mathbb{S}^1} + \partial_t^2) + V_M$ where $\mathbb{C}/\langle i \rangle$ has been isometrically identified with $\mathbb{S}^1 \times \mathbb{R}$ endowed with the usual product metric $d\theta^2 \times dt^2$, and the potential V_M is the square of the norm of the differential of the Gauss map of M with respect to $d\theta^2 \times dt^2$ (V_M is bounded since M has bounded Gaussian curvature by item 6 of Theorem 5.7). Finally, the kernel of L_M restricted to bounded functions is finite dimensional; this finite dimensionality was proved by Meeks, Pérez and Ros[5] in [30] and also follows from a more general result by Colding, de Lellis and Minicozzi [2]).

As for the proof of property (T2) above, the aforementioned control on the Laurent expansions in poles of u_t coming from the integration of the Cauchy problem for the KdV equation, is enough to prove that the corresponding meromorphic function g_t associated to u_t by equation (25) has the correct behavior in poles and

[5]Following arguments by Pacard (personal communication), which in turn are inspired in a paper by Lockhart and McOwen [17].

zeros; this property together with the fact that both S_M, S_M^* preserve infinitesimally the complex periods along any closed curve in $\mathbb{C}/\langle i\rangle$, suffice to show that the Weierstrass data $(g_t, \phi_3 = dz)$ solves the period problem for every t and has the same flux vector $F = (h, 0, 1)$ as the original M, thereby giving rise to a surface $M_t \in \mathcal{P}$ with the desired properties. This finishes our sketch of proof of the holomorphic integration of the Shiffman function of an arbitrary surface $M \in \mathcal{P}$ satisfying the hypotheses of Theorem 5.10.

Remark 5.11. While the classification problem for properly embedded minimal planar domains stated at the beginning of Section 5 has been completed, a natural and important generalization to it remains open:

> *Problem: Classify all complete embedded minimal planar domains in* $\mathbb{R}^3$.

This more general classification question would be resolved if we knew a priori that any complete embedded minimal surface M of finite genus in $\mathbb{R}^3$ is proper. The conjecture that this properness property holds for such an M is called the Embedded Calabi-Yau Conjecture for Finite Genus. In their ground breaking work in [4], Colding and Minicozzi solved this conjecture in the special case that the minimal surface M has finite topology. More recently, Meeks, Pérez and Ros [23] proved that the conjecture holds if and only it M has a countable number of ends. However, as of the writing of this manuscript, the solution of the Embedded Calabi-Yau Conjecture for Finite Genus remains unsettled.

References

[1] M. Callahan, D. Hoffman, and W. H. Meeks III. The structure of singly-periodic minimal surfaces. *Invent. Math.*, 99:455–481, 1990. MR1032877, Zbl 695.53005.

[2] T. H. Colding, C. de Lellis, and W. P. Minicozzi II. Three circles theorems for Schrödinger operators on cylindrical ends and geometric applications. *Comm. Pure Appl. Math.*, 61(11):1540–1602, 2008. MR2444375, Zbl pre05358518.

[3] T. H. Colding and W. P. Minicozzi II. The space of embedded minimal surfaces of fixed genus in a 3-manifold IV; Locally simply-connected. *Ann. of Math.*, 160:573–615, 2004. MR2123933, Zbl 1076.53069.

[4] T. H. Colding and W. P. Minicozzi II. The Calabi-Yau conjectures for embedded surfaces. *Ann. of Math.*, 167:211–243, 2008. MR2373154, Zbl 1142.53012.

[5] T. H. Colding and W. P. Minicozzi II. The space of embedded minimal surfaces of fixed genus in a 3-manifold V; Fixed genus. *Ann. of Math.*, 181(1):1–153, 2015. MR3272923, Zbl 06383661.

[6] P. Collin. Topologie et courbure des surfaces minimales de $\mathbb{R}^3$. *Ann. of Math. (2)*, 145–1:1–31, 1997. MR1432035, Zbl 886.53008.

[7] P. Collin, R. Kusner, W. H. Meeks III, and H. Rosenberg. The geometry, conformal structure and topology of minimal surfaces with infinite topology. *J. Differential Geom.*, 67:377–393, 2004. MR2153082, Zbl 1098.53006.

[8] U. Dierkes, S. Hildebrandt, A. Küster, and O. Wohlrab. *Minimal Surfaces I.* Grundlehren der mathematischen Wissenschaften 295. Springer-Verlag, 1992. MR1215267, Zbl 0777.53012.

[9] A. Enneper. Die cyklischen Flächen. *Z. Math. und Phys.*, 14:393–421, 1869. JFM 02.0585.01.

[10] C. Frohman and W. H. Meeks III. The ordering theorem for the ends of properly embedded minimal surfaces. *Topology*, 36(3):605–617, 1997. MR1422427, Zbl 878.53008.

[11] F. Gesztesy and R. Weikard. Elliptic algebro-geometric solutions of the KdV and AKNS hierarchies—an analytic approach. *Bull. Amer. Math. Soc. (N.S.)*, 35(4):271–317, 1998. MR1638298, Zbl 0909.34073.

[12] D. Hoffman and W. H. Meeks III. The strong halfspace theorem for minimal surfaces. *Invent. Math.*, 101:373–377, 1990. MR1062966, Zbl 722.53054.

[13] A. Huber. On subharmonic functions and differential geometry in the large. *Comment. Math. Helvetici*, 32:181–206, 1957. MR0094452, Zbl 0080.15001.

[14] W. Jagy. Minimal hypersurfaces foliated by spheres. *Michigan Math. J.*, 38(2):255–270, 1991. MR1098859, Zbl 0725.53061.

[15] S. Khan. A minimal lamination of the unit ball with singularities along a line segment. *Illinois J. Math.*, 53(3):833–855, 2009. MR2727357, Zbl 1225.53009.

[16] S. Kleene. A minimal lamination with Cantor set-like singularities. *Proc. Am. Math. Soc.*, 140(4):1423–1436, 2012. MR2869127, Zbl pre06028355.

[17] R. B. Lockhart and R. C. McOwen. Elliptic differential operators on noncompact manifolds. *Ann. Scuola Norm. Sup. Pisa*, 12(3):409–447, 1985. MR0837256, Zbl 0615.58048.

[18] F. J. López and A. Ros. On embedded complete minimal surfaces of genus zero. *J. Differential Geom.*, 33(1):293–300, 1991. MR1085145, Zbl 719.53004.

[19] F. Martin and J. Pérez. Superficies minimales foliadas por circunferencias: los ejemplos de Riemann. *Gaceta de la RSME*, 6(3):1–27, 2003.

[20] W. H. Meeks III. The regularity of the singular set in the Colding and Minicozzi lamination theorem. *Duke Math. J.*, 123(2):329–334, 2004. MR2066941, Zbl 1086.53005.

[21] W. H. Meeks III. The limit lamination metric for the Colding-Minicozzi minimal lamination. *Illinois J. of Math.*, 49(2):645–658, 2005. MR2164355, Zbl 1087.53058.

[22] W. H. Meeks III and J. Pérez. Conformal properties in classical minimal surface theory. In *Surveys of Differential Geometry IX - Eigenvalues of Laplacian and other geometric operators*, pages 275–336. International Press, edited by Alexander Grigor'yan and Shing Tung Yau, 2004. MR2195411, Zbl 1086.53007.

[23] W. H. Meeks III, J. Pérez, and A. Ros. The embedded Calabi-Yau conjectures for finite genus. Work in progress.

[24] W. H. Meeks III, J. Pérez, and A. Ros. Local removable singularity theorems for minimal laminations. To appear in J. Differential Geom. Preprint available at http://wdb.ugr.es/∼jperez/publications-by-joaquin-perez/.

[25] W. H. Meeks III, J. Pérez, and A. Ros. Structure theorems for singular minimal laminations. Preprint available at http://wdb.ugr.es/local/jperez/publications-by-joaquin-perez/.

[26] W. H. Meeks III, J. Pérez, and A. Ros. Uniqueness of the Riemann minimal examples. *Invent. Math.*, 133:107–132, 1998. MR1626477, Zbl 916.53004.

[27] W. H. Meeks III, J. Pérez, and A. Ros. The geometry of minimal surfaces of finite genus I; curvature estimates and quasiperiodicity. *J. Differential Geom.*, 66:1–45, 2004. MR2128712, Zbl 1068.53012.

[28] W. H. Meeks III, J. Pérez, and A. Ros. The geometry of minimal surfaces of finite genus II; nonexistence of one limit end examples. *Invent. Math.*, 158:323–341, 2004. MR2096796, Zbl 1070.53003.

[29] W. H. Meeks III, J. Pérez, and A. Ros. Limit leaves of an H lamination are stable. *J. Differential Geom.*, 84(1):179–189, 2010. MR2629513, Zbl 1197.53037.

[30] W. H. Meeks III, J. Pérez, and A. Ros. Properly embedded minimal planar domains. *Ann. of Math.*, 181(2):473–546, 2015. MR3275845, Zbl 06399442.

[31] W. H. Meeks III and H. Rosenberg. The maximum principle at infinity for minimal surfaces in flat three-manifolds. *Comment. Math. Helvetici*, 65:255–270, 1990. MR1057243, Zbl 713.53008.

[32] W. H. Meeks III and H. Rosenberg. The uniqueness of the helicoid. *Ann. of Math.*, 161:723–754, 2005. MR2153399, Zbl 1102.53005.

[33] W. H. Meeks III and H. Rosenberg. The minimal lamination closure theorem. *Duke Math. Journal*, 133(3):467–497, 2006. MR2228460, Zbl 1098.53007.

[34] S. Montiel and A. Ros. Schrödinger operators associated to a holomorphic map. In *Global Differential Geometry and Global Analysis (Berlin, 1990)*, volume 1481 of *Lecture Notes in Mathematics*, pages 147–174. Springer-Verlag, 1991. MR1178529, Zbl 744.58007.

[35] J. C. C. Nitsche. *Lectures on Minimal Surfaces*, volume 1. Cambridge University Press, 1989. MR1015936, Zbl 0688.53001.

[36] R. Osserman. *A Survey of Minimal Surfaces*. Dover Publications, New York, 2nd edition, 1986. MR0852409, Zbl 0209.52901.

[37] B. Riemann. Über die Fläche vom kleinsten Inhalt bei gegebener Begrenzung. *Abh. Königl, d. Wiss. Göttingen, Mathem. Cl.*, 13:3–52, 1867. K. Hattendorf, editor. JFM 01.0218.01.

[38] G. Segal and G. Wilson. Loop groups and equations of KdV type. *Pub. Math. de I.H.E.S.*, 61:5–65, 1985. MR0783348, Zbl 0592.35112.

[39] M. Shiffman. On surfaces of stationary area bounded by two circles, or convex curves, in parallel planes. *Ann. of Math.*, 63:77–90, 1956. MR0074695, Zbl 0070.16803.